

Bachelor thesis

Automation of a test setup to characterize scientific CCDs

from: Eric Müller
Date/ Place of birth: 17.09.1985, Jena

Matriculation number: 374118
Course of studies: Precision Engineering (Ba)
Department: SciTec

supervised by: Dipl. Ing (FH) Sebastian Deiries
European Southern Observatory
Karl-Schwarzschild-Strasse, 2
D-85748 Garching bei München

and

Prof. Dr. Martin Schroeck
University of Applied Sciences Jena
Carl-Zeiss-Promenade, 2
07745 Jena

July 2009

During the forthcoming years the Optical Detector Team (ODT) will implement a large number of CCDs in optical instruments for the Paranal and La Silla observatories. An important step in this process is the CCD characterization and optimization that is done after the device is received from the manufacturer. In order to accommodate the new CDDs and to decrease the workload of the existing test bench, a new testing facility is build.

The chosen concept is the result of years of experience in detector testing at ESO. Nevertheless new hardware and software is introduced and the opportunity is provided to measure fundamental detector parameters namely quantum efficiency, conversion factor, dark current, charge transfer efficiency, read out noise, and cosmetic quality in fully automated modes.

It is possible to uniformly illuminate the optical detector over a 100mm diameter with monochromatic light in the wavelength range from 300nm to 1100nm. Accessible parameters are amongst others exposure time (shutter control), light intensity control and measurement, wavelength, bandwidth, and several clock modes to control the charge coupled devices.

Number of pages 57

Number of figures 34

Number of applicable documents 25

Numbering	Topic	Page
Outline		I
Table of contents		II
Acronyms		III
1	Introduction	2
2	Goal	3
3	The MUSE instrument project	4
3.1	Scientific goals	4
3.2	Technical challenges	5
4	The CCD test bench	7
4.1	Requirements	7
4.1.1	General	7
4.1.2	The illumination system	9
4.2	Considerations concerning the setup	11
4.2.1	Light source	11
4.2.2	Imaging optic	11
4.2.3	Optical filters	12
4.2.4	Monochromatic light	14
4.3	Hardware configuration	14
4.3.1	Additional components	19
4.3.2	Completion and fine adjustments	20
4.4	The light path	20
4.5	Software configuration	25
4.5.1	Functional principle	27
4.5.2	The <i>PRiSM</i> software	27
4.5.3	The <i>LabVIEW</i> software modules	28
4.5.3.1	General annotations	28
4.5.3.2	<i>PowerSupply_standalone.vi</i>	29
4.5.3.3	<i>Filter_wheel_standalone.vi</i>	30

4.5.3.4	<i>MSH 301_standalone2.1.vi</i>	31
4.5.3.5	<i>Keythley_6514_standalone2.0.vi</i>	33
4.5.3.6	<i>Keithley 2100 Series Read Single.vi</i>	33
4.5.3.7	<i>ESP300_standalone.vi</i>	34
4.5.3.8	<i>Pulpo1_standalone2.0.vi</i>	35
4.5.3.9	<i>JUMO_standalone2.0.vi</i>	38
4.5.3.10	<i>USB Interface Board_standalone2.0.vi</i>	39
4.5.3.11	<i>FIERA_standalone.vi</i> and <i>NGC_standalone.vi</i>	40
4.5.4	Automated data acquisition	43
4.5.5	Data reduction and results	48
5	Measurements and results	50
5.1	Wavelength accuracy	50
6	Discussion	55
6.1	Light performance	55
6.2	Additional shutter	55
6.3	Wavelength adjustments	56
6.4	Uniformity of illuminance	56
7	Conclusion	57

Applicable documents

Table of figures

Annex I: Custom-made products

Annex II: Characteristics of components

Annex III: Detector test report

Declaration on autonomy

Abstract

Acronyms

CAD	-	Computer Aided Design
CCD	-	Charge Coupled Device
CPA	-	Image file format for lossless compression of FITS images
DC	-	Direct Current
ESO	-	European Southern Observatory
FIERA	-	Fast Imager Electronic Readout Assembly
FITS	-	Flexible Image Transport System
GPIB	-	General Purpose Interface Bus
GUI	-	Graphical User Interface
IFU	-	Integral Field Unit
MUSE	-	Multi Unit Spectroscopic Explorer
NGC	-	New General detector Controller
NI	-	National Instruments
NPL	-	National Physical Laboratory (England)
OD	-	Optical Density
ODT	-	Optical Detector Team
PC	-	Personal Computer
PSF	-	Point Source Spread function
PTB	-	Physikalisch-Technische Bundesanstalt
SPARC	-	Scalable Processor Architecture
Telnet	-	Telecommunication network
USB	-	Universal Serial Bus
UV	-	Ultraviolet
VI	-	Virtual Instrument (a <i>LabVIEW</i> software module)
VLT	-	Very Large Telescope
VME	-	Virtual Machine Environment

E	-	Illuminance
B	-	Luminance
M	-	Magnification
k	-	F-number
k_M	-	F-number of monochromator
f	-	Focal length
D	-	Aperture of lens
λ	-	Wavelength of incident light
m	-	Order of diffraction
R_S	-	Radius of integrating sphere output port
R_D	-	Radius of illuminated area at the CCD position
g	-	Grating constant

1 Introduction

An important step in the process of implementing Charge Coupled Devices (CCDs) in optical instruments for astronomy, is the characterization and optimization of the device after it is received from the manufacturer. A number of measurements of CCD performance involve the uniform illumination of the chip in question with light of a certain intensity level, at a specific wavelength and with a certain spectral bandwidth.

In 1996 the introduction of the detector controller FIERA (Fast Imager Electronic Readout Assembly), developed at ESO, as well as the growing size of the optical detectors, which could not be handled by the existing testing facility at that time, has made the construction of new test bench named Test and Measurement Evaluation Rig (TAMER). Several improvements have been realized to optimize the turnaround time and the precision of the measurements. New detector heads, each accommodating two CCDs, have been manufactured and put in use.

In actual state the new general detector controller (NGC) can also be used to operate the devices. The design provides the possibility to test large detector sizes of 8k x 8k pixels (15 μ m pixels size) or around 200mm diameter. All major CCD parameters namely quantum efficiency, photo response non uniformity (PRNU), readout noise (RON), linearity, dark current, charge transfer efficiency (CTE) and cosmetic defects can be tested in fully automated modes for the most part.

The detector is mounted in the cryostat head and placed behind a quartz window (see figure 3-1). A vacuum pump generates a vacuum of approximately 10⁻⁶mbar and the cryogenic system cools the head down to a temperature of around -120°C. A constant temperature is achieved by heaters operated by a control unit linked to the CCD controller.

Once the device is tested and qualified against the contractual specifications, the configuration of detector and cryostat remains exactly the same and is mounted to the foreseen optical instrument.

CCDs are the essential sensors for almost all astronomical instruments that operate in the visible wavelength range today. An ambitious project, requiring all in all 24 CCD cryostats should serve as an example and is briefly described in 4.

2 Goal

The intention of this thesis is the assembly and the automation of a test setup that allows to characterize scientific CCDs. Therefore the elected hardware needs to be aligned and several components have to be constructed and manufactured.

The determination of fundamental detector parameters requires the automated data acquisition, data reduction and evaluation as well its clear summary. For this purpose routines, that have been used at the existing test facility, needs to be adapted in the way that they can be used to operate the new hardware.

This requires to develop driver software for the several controllers, which should also provide the opportunity to access the test assembly interactively from a remote computer. Furthermore the thesis should serve as documentation about the hardware and the software modules in use.

3 The MUSE instrument project

The Multi Unit Spectroscopic Explorer (MUSE) is a panoramic integral-field spectrograph in development for one of ESOs Very Large Telescopes (VLT) on Cero Paranal in Chile. It combines a wide field of view with an improved spatial resolution, assisted by adaptive optics and operates in the visible wavelength range.

3.1 Scientific goals

Using the unique capability to obtain up to ten thousands of spectra in one single exposure, scientists aim to study the evolution of massive stars and intend to answer a number of key questions about super massive black holes and their impact on the galaxy evolution.

Thanks to their strong hydrogen emission lines, MUSE will be able to detect and study progenitor of galaxies similar to the Milky Way at a distance of more than 10 billion light years. It is expected to discover around 15000 of all types of galaxies. The unique homogeneous set of physical data will be a key element to understand the formation and evolution of galaxies.

In the case of unpredictable events such as the apparition of a new comet and unlike space missions which need to be programmed well in advance, MUSE shall be able to observe the object without delay. Furthermore its spectrographic capabilities will be crucial to study the complex chemical and physical evolution of the comets when they approach our sun.

3.2 Technical challenges

In contrast to classical spectrographs which provide a spectral information of one spatial direction, an integral field spectrograph is designed to give a spectral information of a two dimensional field of view. In order to preferably have a wide field of view, MUSE uses 24 integral field spectrographs that allow to observe an area of 1×1 arcmin². Each unit is equipped with its own cryogenically cooled CCD head accommodating a detector with a size of 4096x4096 pixels of 15 microns.

The VLT secondary mirror is equipped with more than one thousand actuators to remove the distortion due to the atmosphere in real time. Therefore four artificial stars are created by the smaller auxiliary telescopes, to have a reference. This system is part of the VLT adaptive optics facility, developed separately from MUSE, by ESO.

The light gathered by the 8.2m mirror is focused on a field splitter and separator by the adaptive secondary mirror, resulting in 24 different light paths that are directed to each integral field unit (IFU). Within each IFU the field of view is again spilt into 48 slices by the image slicer and finally a detector records the light signal, that has been dispersed by a spectrograph. Each exposure taken by MUSE will have all in all 370 millions of pixels.

ESO is in charge of delivering 24 detector systems, that fulfil the high technological requirements of this ambitious project. To assure highest instrument efficiency and best image quality, each detector system needs to be tested to verify its usability, reliability and stability.

The MUSE instrument CCDs are back-illuminated, deep depletion devices with a graduated anti-reflection coating and manufactured by *E2V*. These science grade detectors of type CCD231-84-4-D76 are customer specific grade chips that meet the ESO requirements described in [1].

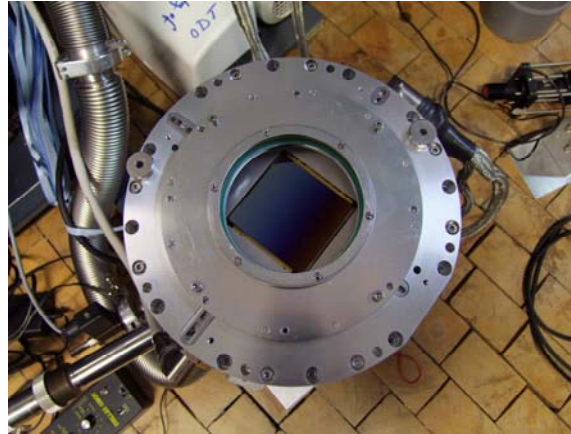


Figure 3-1: The first science grade CCD (named CERES) for MUSE

Due to the increasing number of optical detectors to be characterized and optimized using the existing ODT test bench, the necessity arose to build a new testing facility and the MUSE detectors are only a few of a large number of devices to be tested in the future.

Therefore a design is chosen which is based on the test bench concept introduced, after a long, but fruitful, process of considerations and tests, by Paolo Amico and Thorsten Böhm in 1998 [2]. The concept foresees a monochromator with internal shutter lighted by means of a halogen light source and imaging optic, two filter wheels and an integrating sphere for a uniform, monochromatic illumination of adjustable intensity and exposure time. A monochromator is chosen instead of filters to provide narrow band measurements.

4 The CCD test bench

4.1 Requirements

4.1.1 General

Apart from an acceptable price of all components, the general requirements can be summarized as follows:

- The whole test assembly is foreseen to be mounted on an optical bench in a small laboratory of 5 x 6 m² area
- To guarantee full automated data acquisition using appropriate software, each device or rather controller needs a connection to the test bench PC via a common interface (e.g. GPIB, Serial, USB)
- Uniform control software needs to be developed and existing software modules have to be integrated
- All devices have to be operable in combination and by standalone software modules
- It must be guaranteed that the light path is isolated from the lighting conditions in the test bench room as good as possible and that these conditions do not change (e.g. by turning on the room light) during the measurements
- Both available CCD controllers must be supported

In order to test the fundamental CCD parameters it must be possible to take three different types of exposures at different read out modes.

The readout mode defines the way the CCD is read out including the speed in kpix/s, the ports used, the gain (0.5 e-/ADU for the high gain and 2.5 e-/ADU for the low gain) and in some cases the number of lines to be read.

Flat field exposures require the CCD to be illuminated with uniform light of a specific wavelength for a definable exposure time. Therefore a monochromatic and homogeneous light source is needed as well as a shutter to exactly adjust the time of exposure.

The detector is intentionally not illuminated, if a bias exposure is taken. For this purpose the integration time is set to zero seconds and the CCD read out procedure starts immediately. Roughly speaking, this type of image is also a flat field image without having an exposure time. The noise due to the temperature in the resulting image is insignificant. The only recorded “signal” is the noise of the readout amplifier.

For the purpose of taking a dark acquisition (dark image) a cover has to be mounted onto the CCD head to make sure that no light reaches the CCD. After a specific integration time the detector is read out. This image contains information about the noise due to the temperature as well as the readout noise of the amplifier. In addition disruptive events like cosmic rays are detected.

A time delayed integration exposure starts by reading out the CCD with the shutter closed. During the readout the shutter is opened to illuminate the CCD with uniform, monochromatic light, as if a flat field image is taken. Taking the exposure ends, as soon as the readout has finished. The resulting image is divided into three parts the bias area at the bottom (where the output register is located), the area where the luminous gradient is present and the saturated area at the top of the image.



Figure 4-1: Time delayed integration (TDI) image of a 4096x2048 pixel detector

4.1.2 The illumination system

The requirements mainly depend on the chosen monochromator. The aperture ratio and the size of its slits determine the parameters of the optic and the size of the light source.

The essential wavelength range of the broad band light source needed, is given by the sensitivity of the CCDs to be tested. The lower wavelength limit is 300nm and the upper limit is 1100nm. Furthermore a temporally and spatial stability of light intensity and a smooth continuum without spectral lines is required as well as a sufficient light output especially in the UV range, to be able to illuminate the detector over the whole range from a few ADU to saturation at acceptable low exposure times. In addition the size of the light source needs to be big enough, to have an image of sufficient size in the plane of the monochromator input slit, when it is imaged by an additional optic.

The imaging optic must efficiently collect the light emitted by the source and image the source (e.g. filament) magnified onto the monochromator input slit. Also the aperture ratio of the imaging beam should meet the requirements of the chosen monochromator in order to maximize the efficiency. The material of the lenses must transmit the whole spectrum especially the weak UV light as already mentioned.

Furthermore the transmission needs to be adjustable in preferably small and equidistant steps from 100% to 1%, to keep the exposure times in a reasonable range and disruptive orders of light of certain wavelengths have to be disabled by optical filters in case a diffraction grating is used to produce monochromatic light. Moreover the selected filter glass must not delimit the wavelength range from 300nm to 1100nm.

The core of the test assembly, a monochromator, must have input port and output port aligned, to ensure to have a compact test setup, which can be mounted on a preferably small optical bench. In addition a second output port is required, to provide the opportunity to couple light into a fibre, that allows to illuminate the detector punctual with monochromatic light (PSF experiment). The gratings efficiency has to be optimized for the UV part of the spectrum. A wavelength accuracy of ± 1 nm and a bandwidth adjustable to a minimum of 4nm is sufficient for the measurements to be done.

An uniform illumination over the whole chip (4kpix x 4kpix of 15 μ m size equals an diameter of ~100mm) is intended to be achieved by an integrating sphere attached to the monochromator output slit, where the uniformity should not vary by more than 3%. Moreover there must be an opportunity to measure the photocurrent in the sphere (e.g. for QE measurements). In order to illuminate the CCD for a definable period of time an electronic shutter is suitable.

As mentioned above the opportunity is required, to illuminate the CCD with a point light source at arbitrary positions and wavelengths within the mentioned range. For this purpose a light tight work area between integrating sphere and detector is needed, which also has the advantage to be able to mount an image projector in front of the chip.

For the purpose of absolute flux calibration of the system [3] or in other words, to be able to monitor the photon flux at the CCD surface during a series of measurements (necessary for QE measurements for example), you have to know the ratio between the flux at the

CCD surface position (can not be measured in this place when the detector is mounted) and another location in the light path, preferably inside the integrating sphere. This requires two photodiodes [3], one permanently mounted to the integrating sphere and a further one, which is only used for the test bench calibration. Therefore the CCD cryostat is replaced by this diode, which is attached to a special flange (already exists) for the duration of this procedure.

4.2 Considerations concerning the setup

4.2.1 Light source

In order to get light into a monochromator and considering the spectrum to be covered by the source, halogen lamps and arc lamps come into consideration. Halogen lamps have a more stable intensity, considered over time, compared to arc lamps and an appropriate power supply should allow to keep the power of the source constant, which contributes to improve the stability. Furthermore halogen lamps are continuum radiation sources with a relatively small spectral variance of intensity. The minimum size of the light source can roughly be calculated, if the magnification of the optic and the size of the monochromator input slit are known.

4.2.2 Imaging optic

Quality and quantity of the light leaving the monochromator tremendously depends on how the light is coupled into the device. A maximum efficiency can be achieved by magnified imaging (input port area is generally larger than the area of the spiral-wound filament) of the filament onto the input slit, by a condenser optic and a collective lens, which provide a light beam with an opening ratio equal to the required opening ratio of the monochromator. The ratio is usually described by the F-number of the device.

Several manufacturers offer completely assembled kits for that purpose, but it is preferred to have a modular and therefore easy expandable and modifiable assembly of commercial products, that meet the requirements soonest. The relative aperture of a condenser is a good measure for its efficiency to collect light and it equates to the focal over diameter ratio ($k=f/D$) in a good approximation. One should not forget that it is essential to find a compromise between a preferably small F-number, allowing to collect a bigger amount of light and little spherical aberration, which increases by smaller F-numbers.

The minimum aperture of the additional collective lens equates the aperture of the condenser or contrariwise and the focal length of the focusing lens is given by the monochromators maximum angle of aperture ($f = D \cdot k$). UV-grade fused silica is suitable as a material for the lenses in order to not limit the desired spectrum.

4.2.3 Optical filters

An advantageous solution to remotely control the intensity level, is the use of neutral density filters with different transmissions (optical densities) that are put into the light path by means of a filter wheel with an appropriate controller. Very low light levels can be achieved at respectable exposure times. The aperture must always remain the same, independent from the filter position (also in case there is no filter mounted for a transmission of 100%), to not additionally adjust the intensity by differing fading.

Since a reflexion grating mounted to a monochromator is intended to be used to produce monochromatic light, it is possible that the light at the output slit is not monochromatic, but a mixture of the desired wavelength (first order of diffraction) and a further second order wavelength (and higher orders). This must be avoided and the disruptive wavelength must be blocked by coloured glass filters, used as order sorting filters. According to the equation of reflexion gratings [24]

$$\sin \beta = -\left(\frac{m \cdot \lambda}{g} + \sin \varepsilon\right) \quad (4.1)$$

Variables:

- β - Angle of reflexion with respect to the grating normal
- ε - Angle of incidence with respect to the grating normal
- λ - Wavelength of incident light
- m - Order of diffraction
- g - Grating constant

the angle of reflexion remains the same for different wavelengths of the incident light and other orders of diffraction. The zeroth order corresponds to the reflected light, where the first order of diffraction corresponds to the desired wavelength.

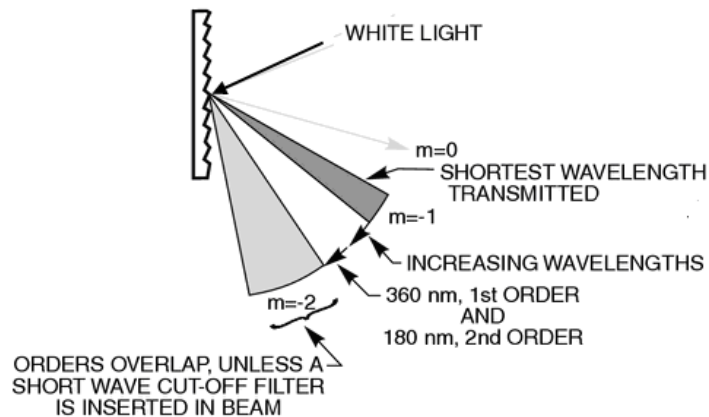


Figure 4-2: Polychromatic light diffracted by a grating [14]

The outcome of this consideration is the following. It has to be verified that half the desired wavelength is blocked either by the system (spectrum of light source) or by proper optical filters.

4.2.4 Monochromatic light

Narrow band measurements at low stray light and adjustable bandwidth are intended to be done in an automated way, different light paths (axial and lateral) are foreseen and the complete setup needs to be isolated from the room light conditions. All these features are combined in a monochromator.

An integrating sphere mounted at the monochromator output port affords to have diffuse light output and a uniform intensity contribution in the plane where the detector is placed.

An iris shutter with a proper aperture (in case of dazzling effect) is suitable for the task, to accurately determine the exposure time. A constant low light level inside the test bench room can be achieved by reading and regulating the room light level, using a further photodiode in combination with an electrometer and appropriate hardware and software to control the room light.

4.3 Hardware configuration

All devices that have an impact on the light path are mounted on a *Thorlabs* 1800mm x 750mm optical table. Additional components allow to uplift the mentioned devices onto the optical axis in 235mm height (see 4.3.1).



Figure 4-3: The new CCD test bench

All main components along the light path are described in the following. The **light source system** consists of a *Newport 60000 Series Q* Housing (air-cooled by a fan wheel) and a horizontal mounted 100W quartz tungsten halogen lamp (*QTH* model 6333, see figure II-9 in the annex for spectral irradiance). An along the optical axis adjustable condenser (F/1.5) and an additional collective lens, made of standard quartz, are used to image the filament on the vertical monochromator slit. The *Newport* model 69931 power supply provides constant power operation, which is required for the measurements. It is linked to the test bench PC via RS-232 interface to allow remote control.

There are three identical *Newport filter wheels* (model 74041), one linked to and operated by the monochromator and two of them operated by their own controller unit. Each wheel can hold up to six filters of 25.4 mm diameter, but there is always one holder without a

filter (aperture stays the same) mounted, to afford unfiltered light throughput. The first two filter wheels hold neutral density filters (ND-filters) from *SCHOTT* with transmissions of 71% (mounted twice), 50%, 25%, 10%, 5%, 2.5%, 0.5%, 0.1% and 0.025% to allow the adjustment of the transmission from 100% to 0.00126% in 28 steps (see figure II-5 for transmission curves and figure II-4 in the annex for detailed information about the mounted filters). This is done by combining (adding) the optical densities of two filters that are put into the light path one after another. The software automatically adjusts the filter wheel position according to the chosen density. In the third filter wheel the *SCHOTT* order sorting filters *305FG01-25*, *550FG05-25* and *FSR-RG1000* are mounted, having cut-off wavelengths at 305nm, 550nm and 1000nm (see figures II-1, II-2 and II-3 in the annex for transmission curves). The monochromator as well as the filter wheel control units are connected to the test bench PC via GPIB interface.

The *Newport MSH 301 ¼ M monochromator* has a 600 l/mm plan grating mounted with a blaze-wavelength of 400nm for increased efficiency in the UV range (see figure II-6 in the annex for typical efficiency of ruled gratings with similar blaze wavelength). The device is set up for a wavelength range from 250 to 1300 nm with 0.35 nm accuracy and a minimum band pass of approximately 0.5nm and houses an internal shutter at its input port. A motorized slit is mounted at each of the three ports (*Newport* models *74115*, *74117*, *74118*). The device is linked to the PC via GPIB interface.

The *LOT-ORIEL K-200W-SP integrating sphere* has a diameter of 200mm with two aligned 40mm diameter main ports and an integrated stray light shield, avoiding the light going directly from the input to the output. The internal BaSO₄ coating ensures a reflectance better than 96% in the range from 400nm to 1100nm and better than 95% in the UV range from 320nm to 400nm (see figure II-7 and figure II-8 in the annex). A *Hamamatsu* 1cm² silicon photo diode, calibrated by reference to NPL and PTB standards, is connected to the first *Keithley* electrometer *KE 6514* (used as ammeter) by a low noise triax cable and mounted to an additional port near the output port to measure the flux in the sphere. In the lower measurement range of 2nA the resolution of the *KE 6514* is 10fA.

The *Prontor Magnetic E/64* iris **shutter** has a custom made shutter housing and shutter driver and is controlled by PULPO (via TTL signal), a temperature and pressure controller developed at ESO. The maximum aperture of the shutter is 64mm and the minimum exposure time 30ms.

A customized wooden light tight box with the mentioned shutter mounted inside, allows to operate a XYZ linear stage in a light tight environment and to have direct access to the entrance window of the CCD head (e.g. for cleaning purposes). An image projector can be mounted onto the CCD head easily in this configuration.

The XYZ linear stage holds a point light source (light coming from second output port of monochromator via fibre cable) and consists of three linear stages from *Newport (M-ILS50CC, M-ILS150CC and M-ILS250CC)* only differing in their travel range which is 50mm, 150mm and 250mm. The guaranteed accuracy of each translation stage is five microns and all axes are controlled by the *Newport ESP 300* motion controller, which is connected to the test bench PC via GPIB interface. The translation stage and the point light source are currently in use at another test setup and therefore not available at present.

A photo diode, linked to a *Keithley* electrometer of the type *KE 2100*, is used to make a statement about the room light conditions from a remote site by reading the voltage and comparing it with a predefined voltage, which is obtained at the light level limit. In the 100mV range the resolution of the *KE 2100* is 0.1 μ V and it is linked to the test bench PC via USB interface.

Using the USB interface board *VM110 (Velleman Inc.)* allows to control the room light (turning on and off), the warning light at the entrance of the test bench room as well as the lock status of the door (locked/ unlocked). It is wired with the electronics of the door latch and the electronics of the lighting.

Finally there is the CCD cryostat which is linked to the CCD controller, either the FIERA or the NGC. The controller generally consists of the detector head electronics, DC power supplies and the embedded computer provided with a *VME SPARC* station, which allows reading the CCD ports in serial and parallel at low noise and various speeds and gains.

There are two **temperature and pressure controller** available to control the temperature and the vacuum inside the CCD head, which is absolutely necessary due to differing behaviours of the CCD parameters at different ambient conditions. The *JUMO Imago 500* is a commercial product, where PULPO is an ESO development as mentioned.

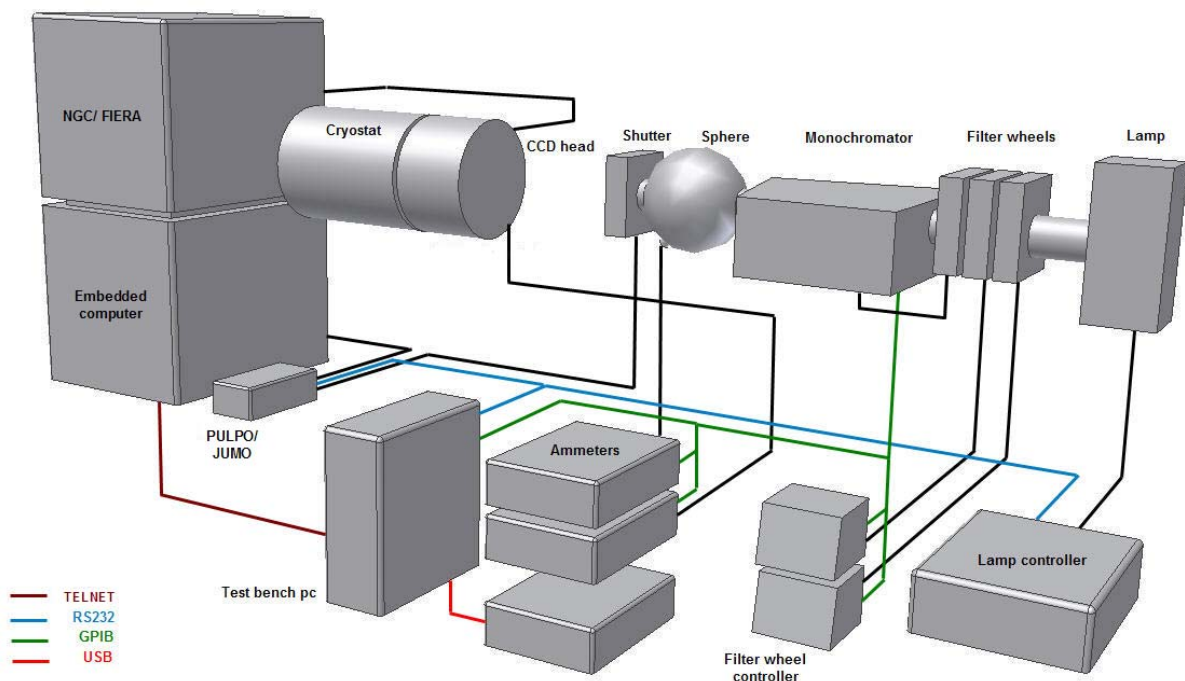


Figure 4-4: CAD model of the test bench components with an impact on the light path including their controllers

4.3.1 Additional components

Several custom-made products are installed at the test bench to align all devices on an optical axis (number I, VIII, IX, see figure 4-5) and to guarantee the partition of the light path from outside (number II, III, see figure 4-5). Furthermore a metallic cover (number VI, see figure 4-5) mounted onto the CCD head for dark exposures, a flange to mount an image projector (number VII, see figure 4-5) and a wooden light tight box (number X, see figure 4-5) was built.

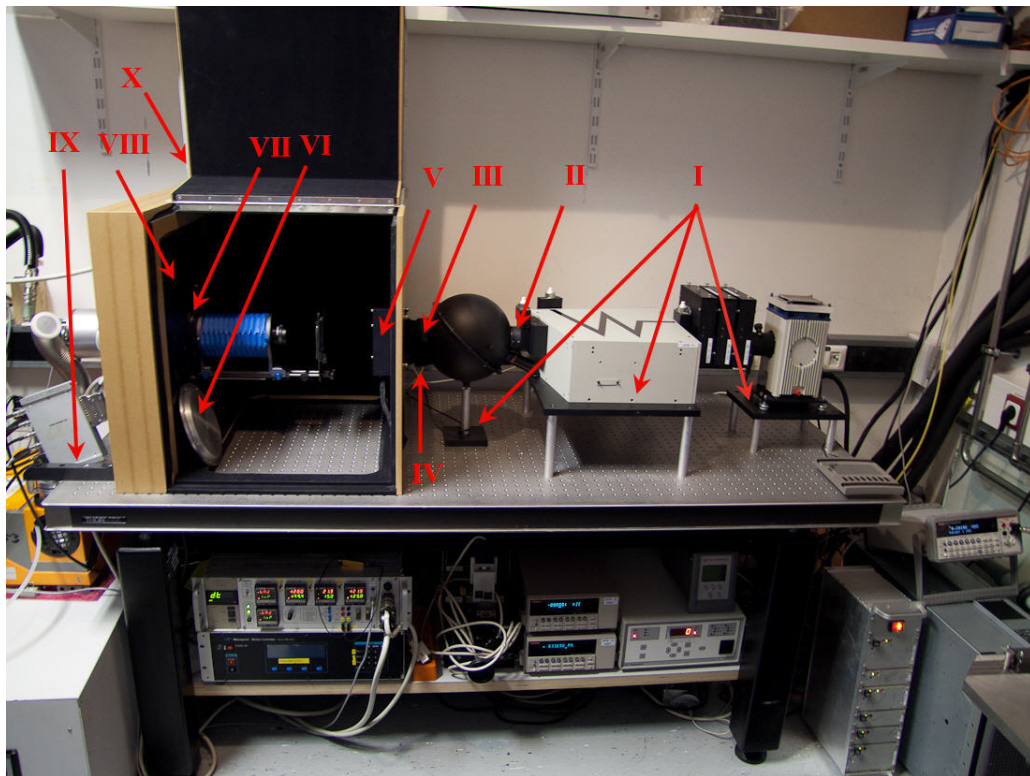


Figure 4-5: Custom-made components at the test bench

Part IV in figure 4-5 consists of an outer ring, which is attached to the integrating sphere and an inner ring holding the photodiode in position. Part VIII is designed to hold different types of cryostats with varying positions of the screw threads. A CAD model of the

constructions, showing more details, can be found in the annex I. The incomplete dimensioning of the CAD models should only reflect the proportions of the models.

4.3.2 Completion and fine adjustments

The light source system is preliminary adjusted in the way that the filament is imaged on the monochromator input slit by means of the collective lens and the adjustable condenser, where the lateral positioning of the image in the plane of the slit is done, using the appropriate fine tuning screws at the housing of the light source. In assembled state (see figure 4-3) the photocurrent is measured inside the integrating sphere and the condensers position along the optical axis is varied to find the intensity maximum and therefore the optimal filament image position. For this purpose the monochromator is adjusted to 630nm and the bandwidth to its maximum (slit apertures at its maximum). Black tape is affixed to critical areas, like the junctions between light tight box, the optical table and the cryostat holder to prevent light entering the light tight zone from outside.

4.4 The light path

The light emitted by a 100W quartz tungsten halogen lamp with a coiled filament of 2.3 x 4.2 mm (width x height) in vertical orientation, is collimated by means of a condenser with an aperture of 33mm and a focal length (f_1) of 50mm. A plano-convex lens of the same aperture with a focal length of 150mm (f_2) images the filament of the light source magnified on the monochromator input slit. The transmission can be adjusted and disruptive higher orders of light are blocked by the filters between the imaging optic and the monochromator. The number of filters affecting the light path depends on the wavelength of the light (order sorting filter) and the light level (neutral density filters) needed. Since both lenses have the same aperture, the following equation gives a rough estimation of the magnification (M) of the filament, where lens aberrations (spherical

aberrations, deviations of the focal lengths), effects of diffraction and variations in the focal length, caused by the filters, are ignored:

$$M = \frac{f_2}{f_1} = \frac{150}{50} = 3 \quad (4.2)$$

Variables:

- M - Magnification
 f_1 - Focal length of lens 1 (condenser)
 f_2 - Focal length of focusing lens 2

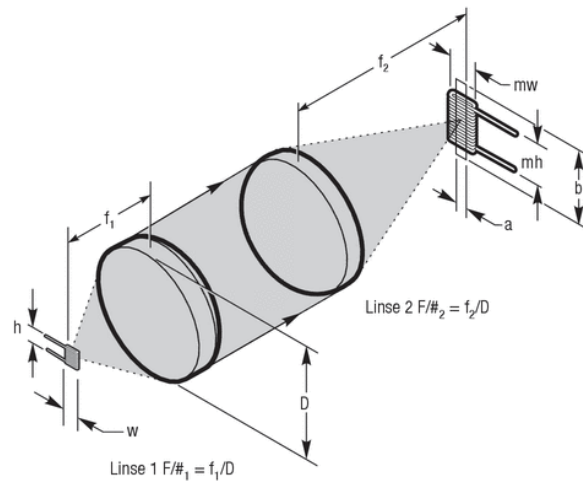


Figure 4-6: Magnified imaging of the filament onto the monochromator input slit by means of the condenser optic (Filters not drawn) [17]

The maximum area of aperture of the *MSH 301* input slit is 3mm x 15mm ($a \times b$, see figure 4-6), but depends on the bandwidth adjusted. Considering the magnification M , the magnified filament theoretically covers an area of approximately 7 mm x 12.6 mm ($mw \times mh$, see figure 4-6) in the focal plane. The measured size of the filament image is 10 mm x 18 mm ($mw \times mh$), which is sufficient to completely illuminate the slit. The holder of the first filter wheel in the light path reduces the useful aperture (D) of the lenses to 30mm and

therefore reduces the opening of the beam coupled into the monochromator to approximately

$$k = \frac{f_2}{D} = \frac{150}{30} = 5. \quad (4.3)$$

Variables:

- k - F-number of imaging optic
 f_2 - Focal length of focusing lens 2
 D - Useful aperture of lens 1 and 2

The monochromator's acceptance angle for light coupled into the device is given by the F-number (manufacturer information) $k_M = 3.9$. Thus the acceptance angle of the *MSH 301* is not completely filled. Its asymmetrical in-plane Czerny-Turner optical configuration is shown in figure 4-7.

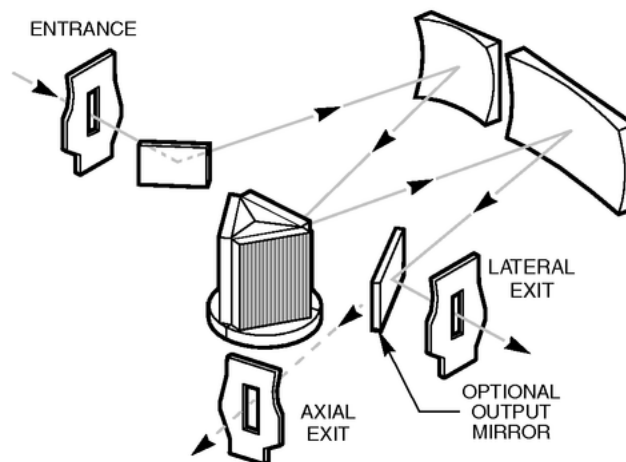


Figure 4-7: The asymmetrical in-plane Czerny-Turner optical configuration of the Newport *MSH 301* monochromator [25]

The light entering the monochromator entrance is dispersed by means of a 600 l/mm plan grating. Depending of its position (free to rotate in a given range), light of a specific wavelength leaves the device either through the lateral exit or through the axial port conditioned by the positioning of the output mirror. The input slit is imaged on the output slit.

In case the light leaves the monochromator at its lateral exit, as shown in figure 4-7, it enters the integrating sphere and is reflected multiple times before it leaves the sphere in the direction to the detector. A tilted baffle prevents light directly passing through the sphere from the input port to the output port as shown in figure 4-8.

At the exit port homogenous, diffuse and monochromatic light of a specific bandwidth is emitted, where the aperture ratio of the light beam is limited by the maximum aperture (64mm) of the shutter.

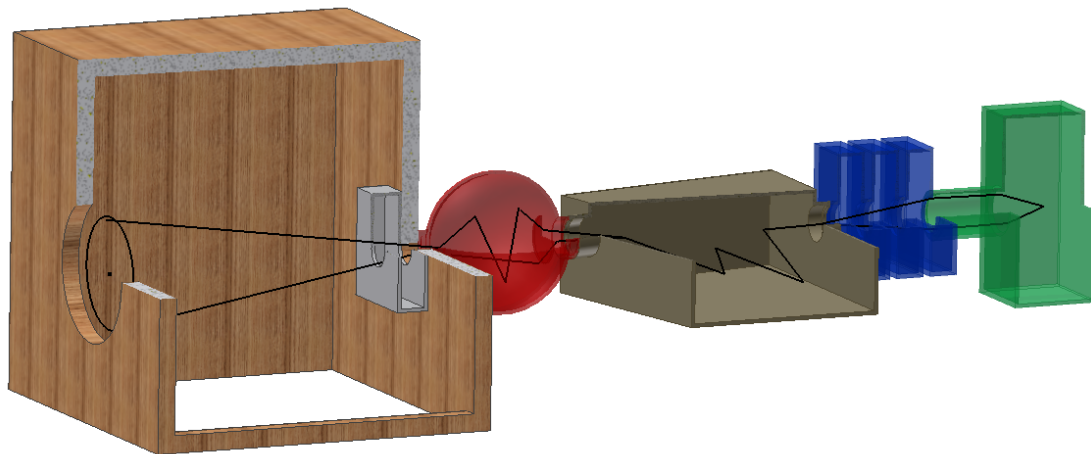


Figure 4-8: The test bench light path

Assuming that the circular area of the exit port radiates according to Lambert's cosine law (Lambertian emitter), the deviation of the illuminance on the chip can theoretically be

determined [4]. The illuminance E depends on the luminance B of the light source (exit port of integrating sphere) and the angle Φ and U' (see figure 4-9) and is calculated as follows:

$$E = \frac{\pi \cdot B}{2} \left[1 - \frac{1 + \tan^2 \Phi - \tan^2 U'}{(\tan^4 \Phi + 2 \tan^2 \Phi (1 - \tan^2 U') + (1/\cos U')^4)^{\frac{1}{2}}} \right] \quad (4.4)$$

The angle U' is given by the distance X (500mm) between detector (on the right) and light source, and the radius of the circular source ($R_S=20\text{mm}$), where angle Φ is given by the distance X and the radius of the illuminated surface. Due to varying CCD dimensions a radius of sufficient size ($R_D=50\text{mm}$) for all 4k x 4k detectors in operation is considered for the calculations.

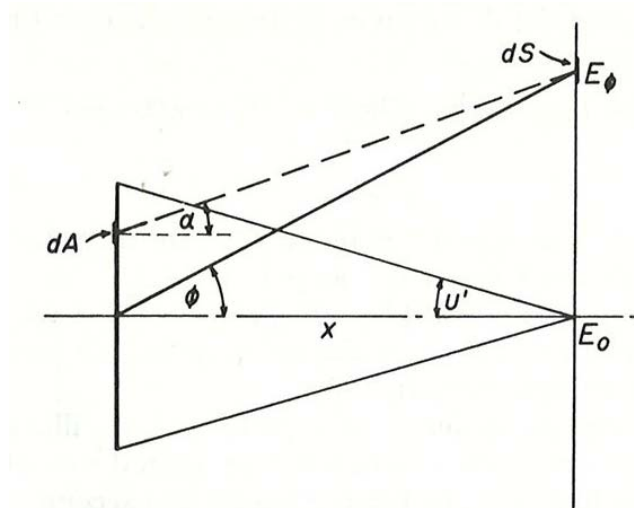


Figure 4-9: Oblique illuminance of the detector (on the right) from a self-luminous disk (output port of the integrating sphere) [4]

The ratio between the illuminance E_Φ and E_0 ($\Phi=0$, see figure 4-9) equals

$$\frac{E_{\Phi}}{E_0} = \frac{1 - \frac{1 + \tan^2 \Phi - \tan^2 U'}{\left(\tan^4 \Phi + 2 \tan^2 \Phi (1 - \tan^2 U') + (1/\cos U')^4\right)^{\frac{1}{2}}}}{1 - \frac{1 - \tan^2 U'}{\left((1/\cos U')^4\right)^{\frac{1}{2}}}} = 0.98 \quad (4.5)$$

Therefore the deviation of the illuminance over the whole CCD theoretically varies by 2%, where the deviation asymptotically approaches to zero from the outer diameter to the optical axis.

4.5 Software configuration

All test bench devices are exclusively operated by *LabVIEW* software. *LabVIEW* is a graphical programming language from *National Instruments*, which is most suitable for developing sophisticated measurement, test and control systems. Interactive or combined operation of the software modules allow, among special and individual tests, full automated CCD characterizations.

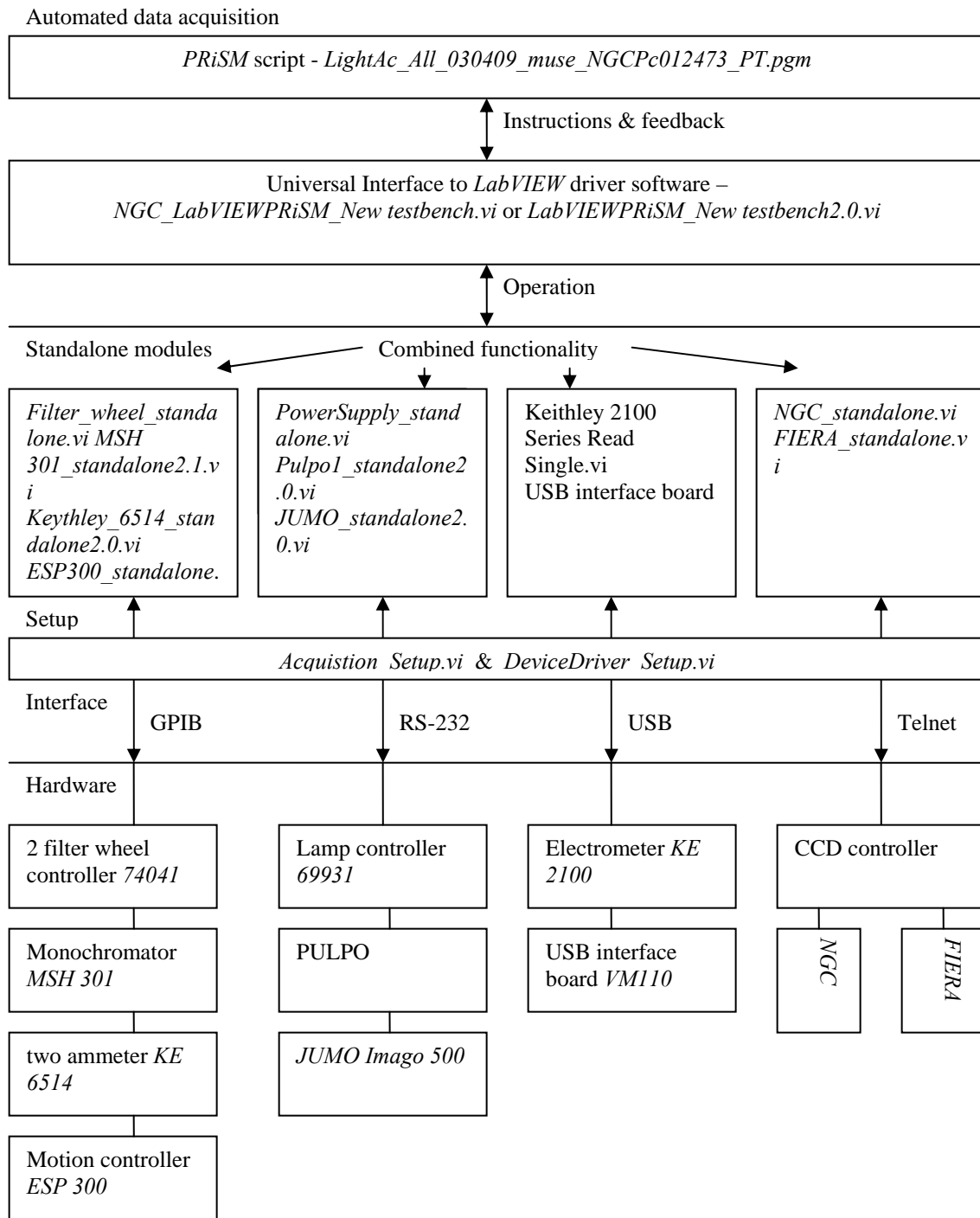


Figure 4-10: Software hierarchy

4.5.1 Functional principle

Each hardware unit can be operated separately by its standalone *LabVIEW* software module as shown in figure 4-10. Two software units, the *Acquisition_Setup.vi* and the *DeviceDriver_Setup.vi*, allow the user to configure the several interface and device specific parameters such as the device address, the number of the sensor to be read out or the password for a remote login as well as basic settings like default directories. The user is asked to refer to the *LabVIEW* modules user manual [5] for a detailed description of these modules.

For the purpose of automated data acquisition a universal piece of *LabVIEW* software exists. It combines the functionality of all standalone units, including the initialization procedure and error handling, reads an assignable text file for instructions and writes the required data into a definable output file. This feature makes it universal, because the text file can be created by any software that meets the requirements as they are described in 4.5.2. Operating two different kinds of software has its reason. In order to acquire data at the existing test bench, *PRiSM* scripts have already been developed to perform all the complex calculations and procedures that are necessary to extract the CCD specific parameters from the raw data.

An automated data acquisition at the test bench is based on a master-slave principle, where the *PRiSM* software acts as master that issues instructions to the *LabVIEW* software (slave) to actuate the hardware. The *LabVIEW* programmes (VI's) are sort of interface between *PRiSM* and the controllers of the test bench devices.

4.5.2 The *PRiSM* software

PRiSM is astronomical software allowing to open and edit the FITS file format, which is the format of the image files produced by the CCD controller, and save it lossless compressed in the CPA format using unsigned 16 bit integer, where the resulting file is only the half of the original file size of approximately 35 megabytes. Furthermore this

software allows to run scripts written in *PRiSM* syntax with the opportunity to take advantage of all the software's features, like image processing and statistical calculations.

The script which is used at the existing CCD test bench has been modified in the way that all the time a test bench device (Filter wheel, monochromator, ammeter etc.) is to be addressed, a text file (*LabPrismin.txt*), containing an appropriate command, is created in a defined directory to access the devices via the *LabVIEW* driver software.

After the execution of a command, another text file (*LabPrismout.txt*), containing a feedback of the success of the operation and the requested information, is created by the *LabVIEW* module. In case an exposure is requested, the resulting image is saved in the location specified in the *Acquisition_Setup.vi*. The types of exposures to be taken by the test bench are mentioned in 4.1.1.

4.5.3 The *LabVIEW* software modules

The standalone modules enable the user to operate each device interactively by remotely connecting to the desktop of the test bench PC. The following description summarizes the functionality of these modules and the way they work. A detailed description of how to use these modules can be found in the *LabVIEW* modules user manual [5].

4.5.3.1 General annotations

Before making use of any software module the user has to make sure that the parameters, concerning the device which is intended to be used, are well-defined in the two existing setup modules (*DeviceDriver_Setup.vi* and *Acquisition_Setup.vi*). When standalone modules are intended to be used, it is necessary to specify the GPIB, RS232 or USB port, depending on the interface of the device to be operated. Therefore the port is selected from a list of available ports located on the respective graphical user interface (GUI). This has only to be done once, if the selection is saved by default and the device address is not changed.

A VI is started by pressing the *Run* button in the upper left (see GUI's). In the following either the GPIB, RS232 or USB interface is configured automatically by applying bus specific parameters, like baud rate or parity for RS232 connections for example. Furthermore the software tries to talk to the addressed controller to verify it is well configured and initializes the device. In case of errors a dialog box appears, providing reasons for the malfunction, otherwise the software is ready to operate.

The red *Abort Execution* button next to the *Run* button should not be used to stop a VI because it interrupts any action and stops the routine immediately. In order to stop it properly the user is asked to press the *STOP* button, usually located in the lower right of the front panel (GUI of a *LabVIEW* programme). A red *busy* indicator is displayed, if the programme is busy. A help window appears when the question mark button is pressed , providing information on the functions of the controls and the values displayed.

4.5.3.2 *PowerSupply_standalone.vi*

This module is used to operate the test bench lamp controller (*Newport* model *69931*) and therefore the power stability of the halogen lamp. Starting the lamp means to initiate a gradual ramp-up to the preset current or power level (*Set level* button). A gradual ramp-down from the preset current or power level is initiated by pressing the *Stop lamp* button. The lamp status (on or off) is indicated by a bright (yellow) or dark (black) circular indicator on the front panel. There is the opportunity to select between two modes, the constant power mode and the constant current mode. All indicators are updated isochronous, if the control *Update* is enabled.

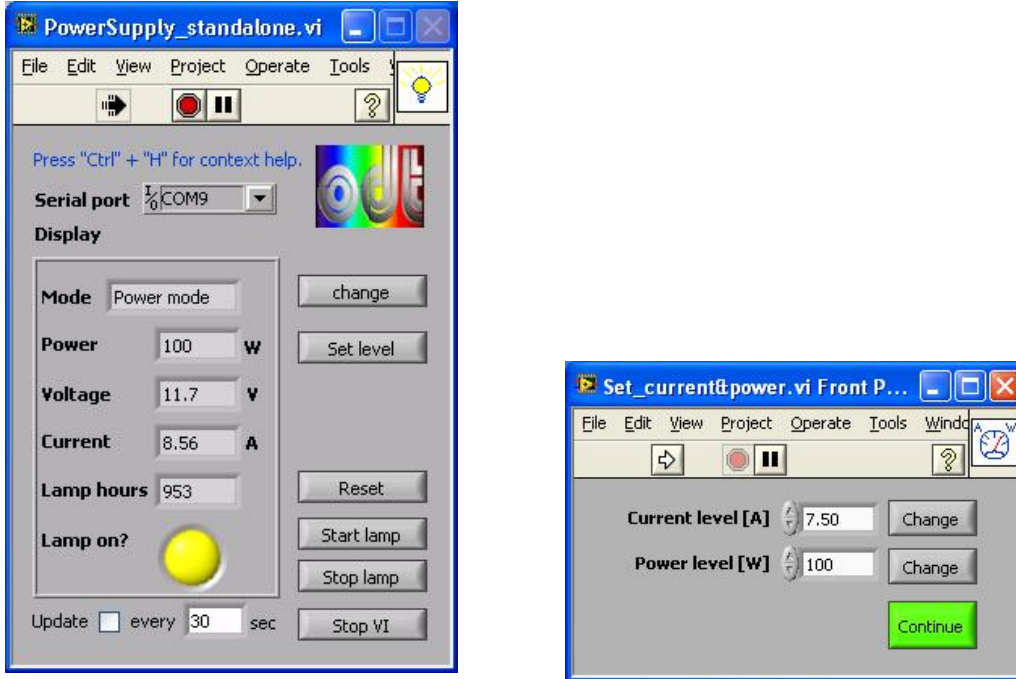


Figure 4-11: The front panel of the *PowerSupply_standalone.vi* (on the left) and the dialog box to set the current and power level

4.5.3.3 *Filter_wheel_standalone.vi*

This VI provides the opportunity to move the two motorized *Newport* filter wheels (the third is operated by the monochromator user interface). A filter is positioned in the light path by pressing the buttons one to six. The *Label* indicators display the density of the filter mounted at each position. Control and indicator turn into light green, when the move is done. A replacement of a density filter of different transmission makes it necessary to change the filter label, which is done by pressing the *Change label* button. In a further dialog box the user can select any label with a maximum number of eight characters for each filter position.

However it is recommended to use the *MSH 301_standalone2.1.vi*, where the functionality of the *Filter_wheel_standalone.vi* is integrated. If the user intends to set a specific density

both filter wheels are operated in combination and the position of both wheels is automatically chosen by the software (assuming that the settings made in the *DeviceDriver_Setup.vi* are well-defined).

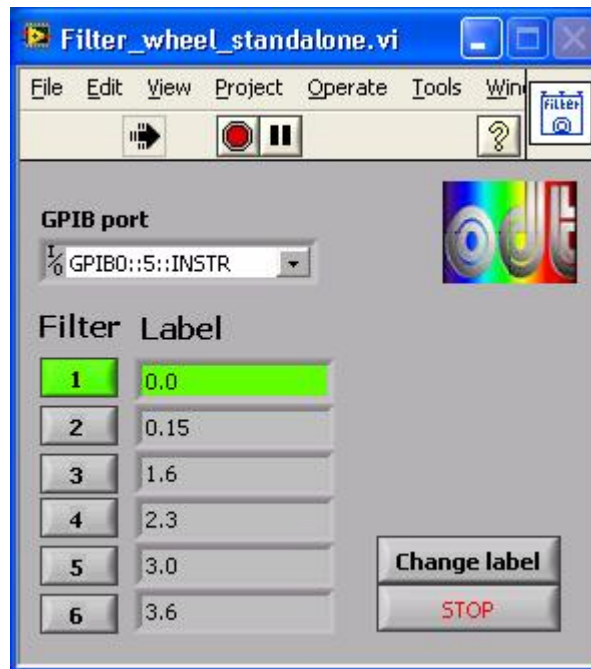


Figure 4-12: Front panel of the *Filter_wheel_standalone.vi*

4.5.3.4 *MSH 301_standalone2.1.vi*

The monochromator can exclusively be operated by driver software. The programme allows to read and adjust the wavelength, bandwidth, order sorting filter, optical density (OD), output port, grating parameters and operating the internal shutter as well. Normally there is no need to set the colour filter because it is done by the routine depending on the selected wavelength and the settings made in the *DeviceDriver_Setup.vi*. According to the current hardware configuration (see 4.3) the filter *305FG01-25* is inserted into the light path at wavelengths greater or equal to 350nm, filter *550FG05-25* is inserted at 580nm and

filter *FSR-RG1000* is inserted at 1050nm for the purpose of blocking the second-order of diffraction (and higher) of half the desired wavelength (see also 4.2.3). All in all 29 different densities from OD 0 to OD 4.9 can be selected from a pull down menu. The two motorized filter wheels, that hold the density filters, are then put in the correct position by the routine.

The grating parameters are usually set by the manufacturer but in case of a memory error, caused by a power outage for example, these parameters, including the number of lines and the offset position of the grating, need to be set to their default values, stated in the technical data sheet delivered with the device. Furthermore it is possible to set the label of the colour filters if they are replaced or after a data loss.

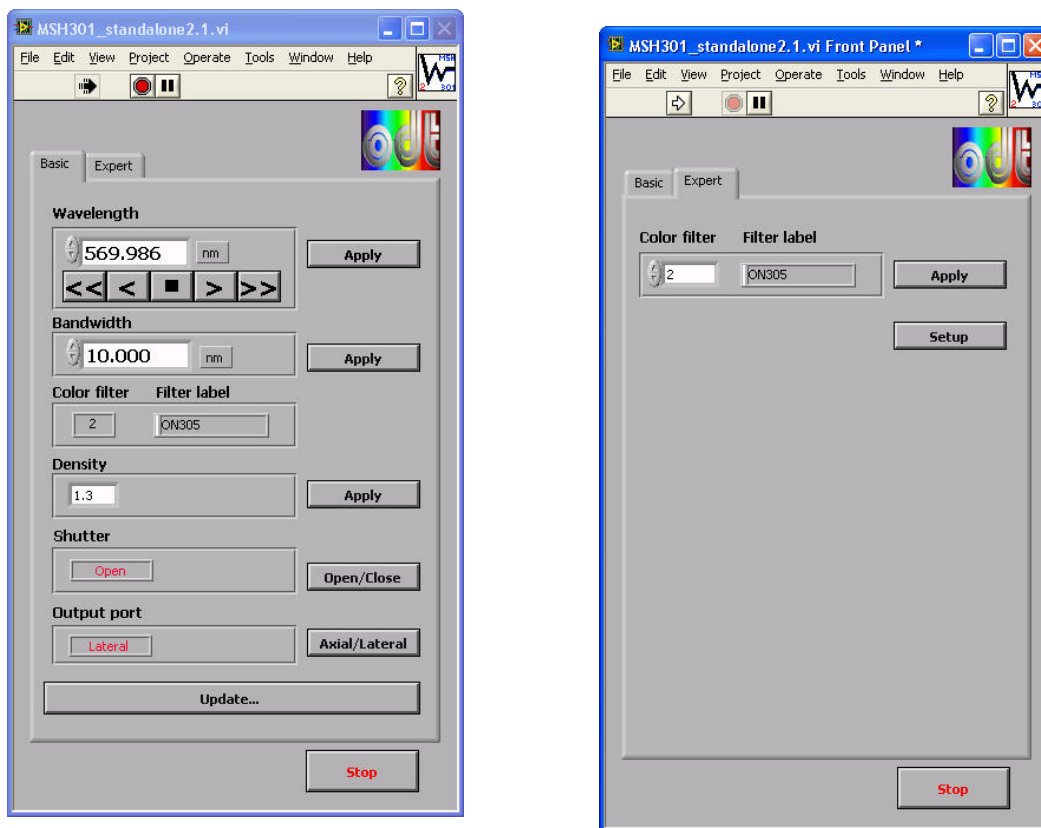


Figure 4-13: Front panel of the *MSH 301_standalone2.1.vi*, with page *Basic* located on the left and page *Expert* (wrong settings can cause malfunction of the device) on the right

4.5.3.5 *Keythley_6514_standalone2.0.vi*

This VI is used to measure the photocurrent of the diode attached to the integrating sphere. Therefore the *Keithley 6514* electrometer is triggered to take a specified number of measurements in series. The mean and its standard deviation are then displayed on the interface in scientific notation. The user has to specify the GPIB device address before running the software. A default value can be set to keep the operating expense in a limit. There is no *STOP* button available because the software stops after having finished the measuring series.



Figure 4-14: Front panel of the *Keythley_6514_standalone2.0.vi*

4.5.3.6 *Keithley 2100 Series Read Single.vi*

The need for determining the light level in the room where the test setup is located, makes it necessary to read the voltage of a further photodiode attached to the *Keithley 2100 Multimeter*. This device driver is basically intended to be integrated into the automated data acquisition software to immediately take action (turns room light off) in case of changing light levels. But if manual measurements are done the voltage can at least be interactively

read and compared to the value settable in the *DeviceDriver_Setup.vi*, which corresponds to the voltage read when the room light is turned off. The USB port of the electrometer is set before the VI is started as well as the number of measurement to be done. The user can select from a list (*Function*) what kind of reading to perform.

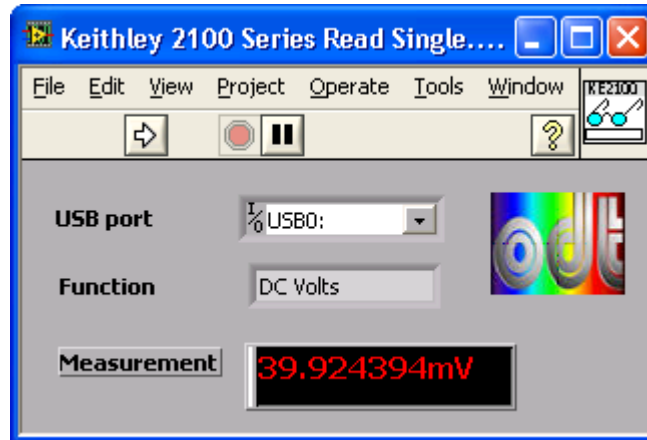


Figure 4-15: Front panel of the *Keithley 2100 Series Read Single.vi*

4.5.3.7 *ESP300_standalone.vi*

Up to three linear stages attached to the *Newport ESP 300* motion controller can be operated by this module. Each axis is dedicated to a page on the front panel where absolute positions can be approached, incremental steps of definable size and direction can be performed and axis specific settings, namely velocity and acceleration (equates to the deceleration as well), are configurable. At each point along the travel range the position of all axes can be reset to zero (*Define home* button). This zero point is approached, when the *Search for home* button is pressed.

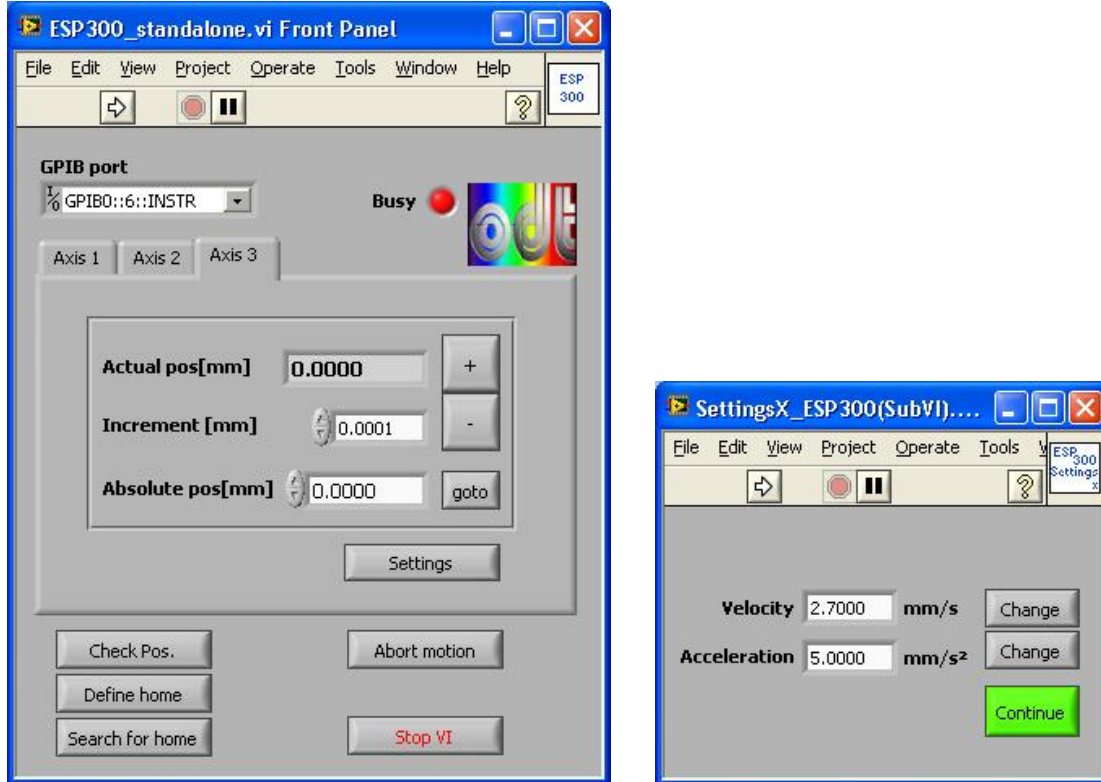


Figure 4-16: The user interface of the *ESP300_standalone.vi* (on the left) and the window to set axis velocity, acceleration and deceleration

4.5.3.8 *Pulpo1_standalone2.0.vi*

Using this software the temperature, pressure and shutter controller PULPO can be actuated. On the page *Table* the parameter and values of all connected sensors (up to seven sensors) and heaters (all in all three heaters attached) are displayed. On page *Chart* the values are plotted with an update period specified on the *Controls* page, where the user can also select to save the gathered data isochronous. Furthermore it is possible to set the temperature trip point of all sensors for the alarm (audio signal in case temperature exceeds this point) and the set point for the attached heaters. An initialisation of the controller (comparable to power cycle the device) is performed, when the *Init* button is pressed.

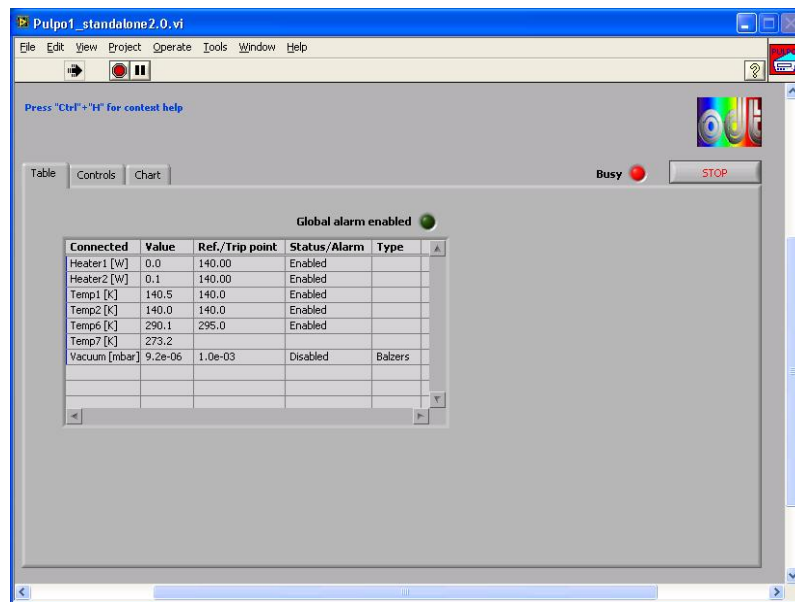


Figure 4-17: Page *Table* of the front panel of the *Pulpo1_standalone2.0.vi*

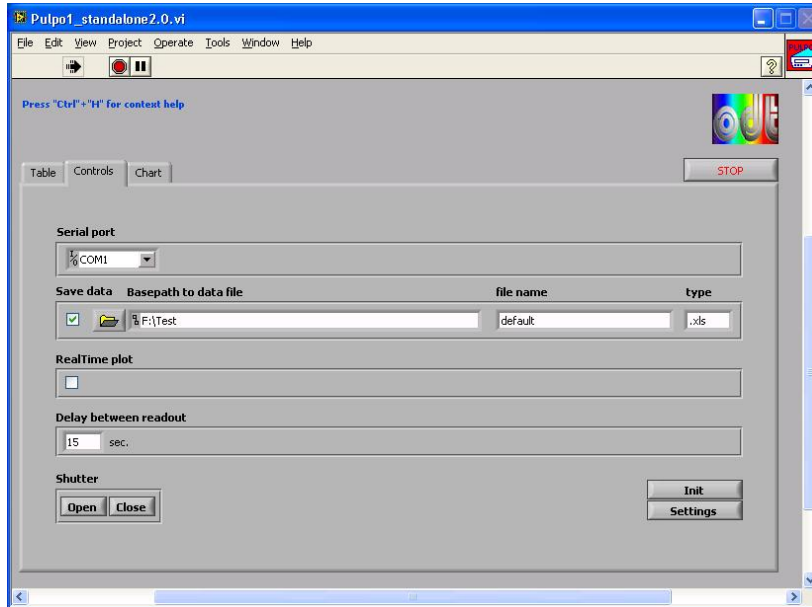


Figure 4-18: Page *Controls* of the front panel of the *Pulpo1_standalone2.0.vi*

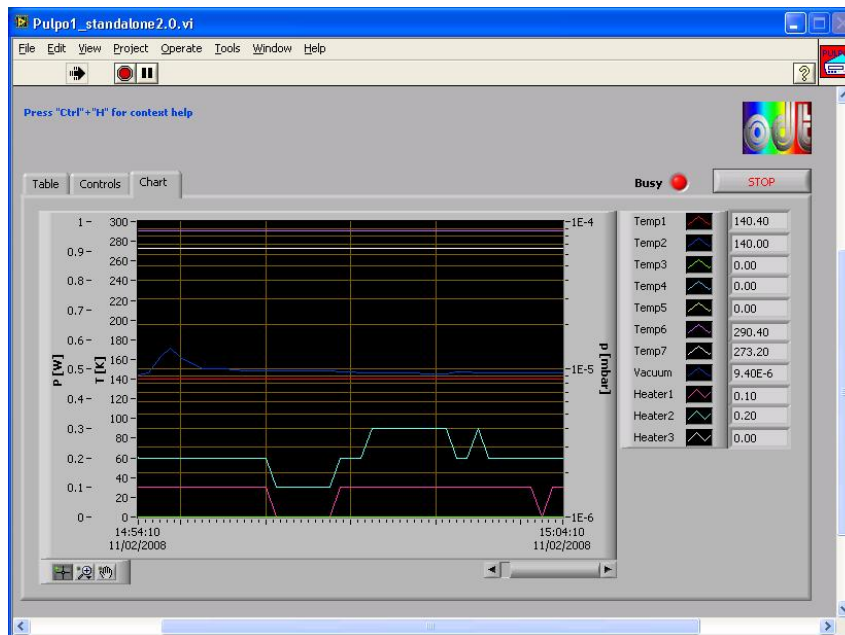


Figure 4-19: Page *Chart* of the front panel of the *Pulpo1_standalone2.0.vi*

4.5.3.9 *JUMO_standalone2.0.vi*

Up to two *JUMO Imago 500* multi-channel process and profile controller can be operated in parallel using this piece of software. The data namely the vacuum and the temperature inside the cryostat head is read, plotted and written to a data file if desired. On page *Controls* the serial port and the slave address has to be specified before the software is started. The update period of the indicators (located on page *JUMO 1* and *JUMO 2*), and therefore the period of time between to sets of data are saved to the specified file, is also configurable. If required the device dependent set point parameters can be set on the pages *JUMO 1* and *JUMO 2*.

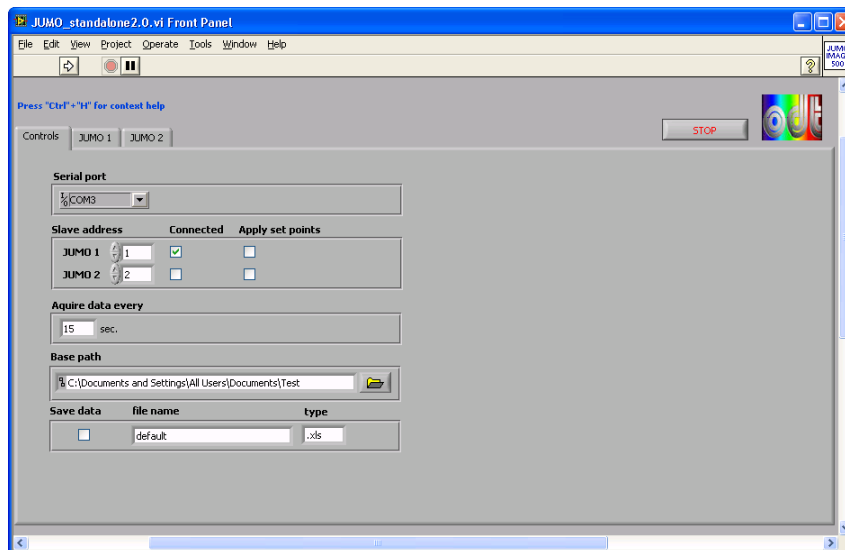


Figure 4-20: Page *Controls* of the *JUMO_standalone2.0.vi* front panel

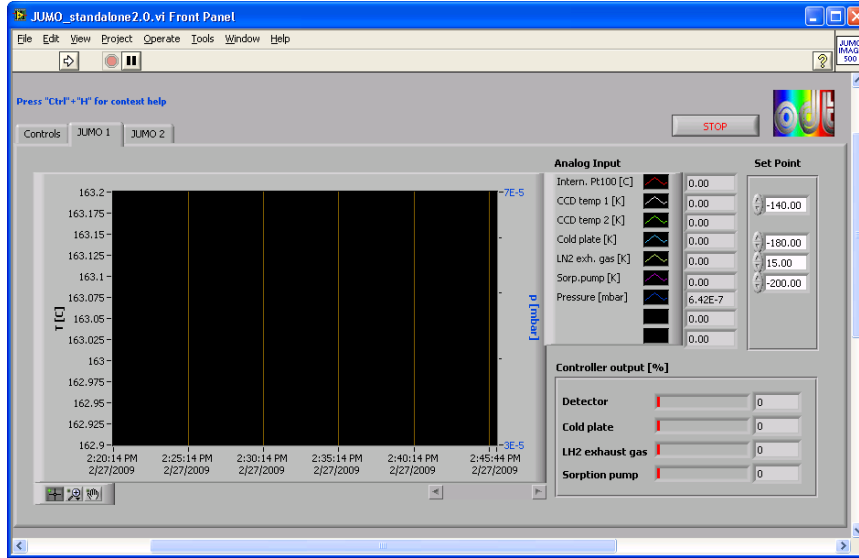


Figure 4-21: Page *JUMO 1* of the *JUMO_standalone2.0.vi* front panel which displays the values of the sensors connected to the first unit

4.5.3.10 *USB Interface Board_standalone2.0.vi*

This software provides the features to operate the test bench warning light, to turn the room light on and off, to lock and unlock the test bench door and the determination, if the door is opened or closed. A dynamic link library (DLL) is provided by the manufacturer (*Velleman Inc.*) to operate the USB interface board, which is embedded into the *LabVIEW* code. The user selects the task from a list and runs the VI. The circular indicator on the front panel shows if the door is opened (dark green) or closed (light green), after the *Door closed?* task has been executed.



Figure 4-22: Front panel of the *USB Interface Board_standalone2.0.vi*

4.5.3.11 *FIERA_standalone.vi* and *NGC_standalone.vi*

The functionality of the two pieces of software is almost the same, they only differ in the syntax of the commands sent to the embedded, UNIX based computer of the CCD controller. Although the *FIERA_standalone.vi* is mentioned only the following description can be applied to the *NGC_standalone.vi* as well. All necessary functions to interactively take exposures are combined within this module. After having started the software it opens a telecommunication network (telnet) connection to the mentioned UNIX based computer, logs in automatically, using the parameters specified in the *DeviceDriver_Setup.vi*, and reads its operational state which is either *online* (ready to use), *standby* or *off*. The buttons in the lower section of the GUI are used to exert influence on the operational state. On page *Setup* essential parameters to take an exposure at the test bench can be set, namely the type of exposure (see 4.1.1), the exposure time, the readout mode (see 4.1.1), the number of exposures and their name in case they are intended to be saved. If desired, the image can be displayed and edited in a window appearing after the exposure has been taken (see figure 4-25). In addition PULPO can be read out and the temperature as well as the pressure,

predominating in the detector system, is displayed on page *Indicators*. Commands sent to and responses received from the embedded computer are logged in the *Telnet log*.

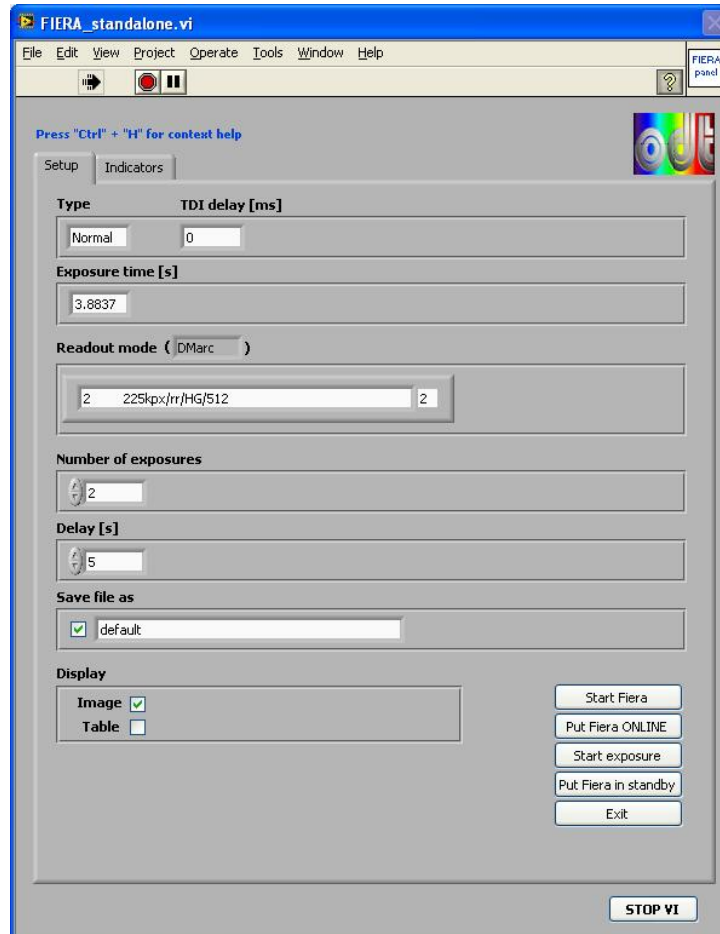


Figure 4-23: Page *Setup* of the *FIERA_standalone.vi*

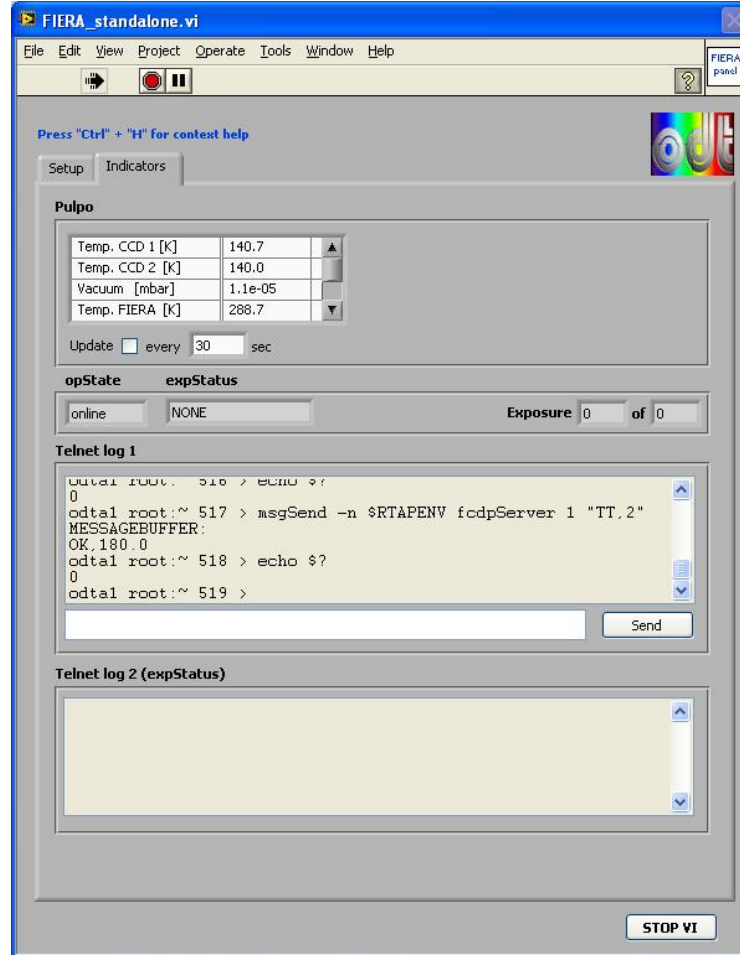


Figure 4-24: Page *Indicators* of the *FIERA_standalone.vi*

Not only the image can be displayed but also the pixel table (containing the values of each pixel) and the FITS image header (contains image specific information like exposure time, number of pixels and recording time). Therefore an open source *LabVIEW* library named *GFITSIO*, developed at the *U.S. Naval Research Laboratory*, was implemented into the *FIERA_standalone.vi*.

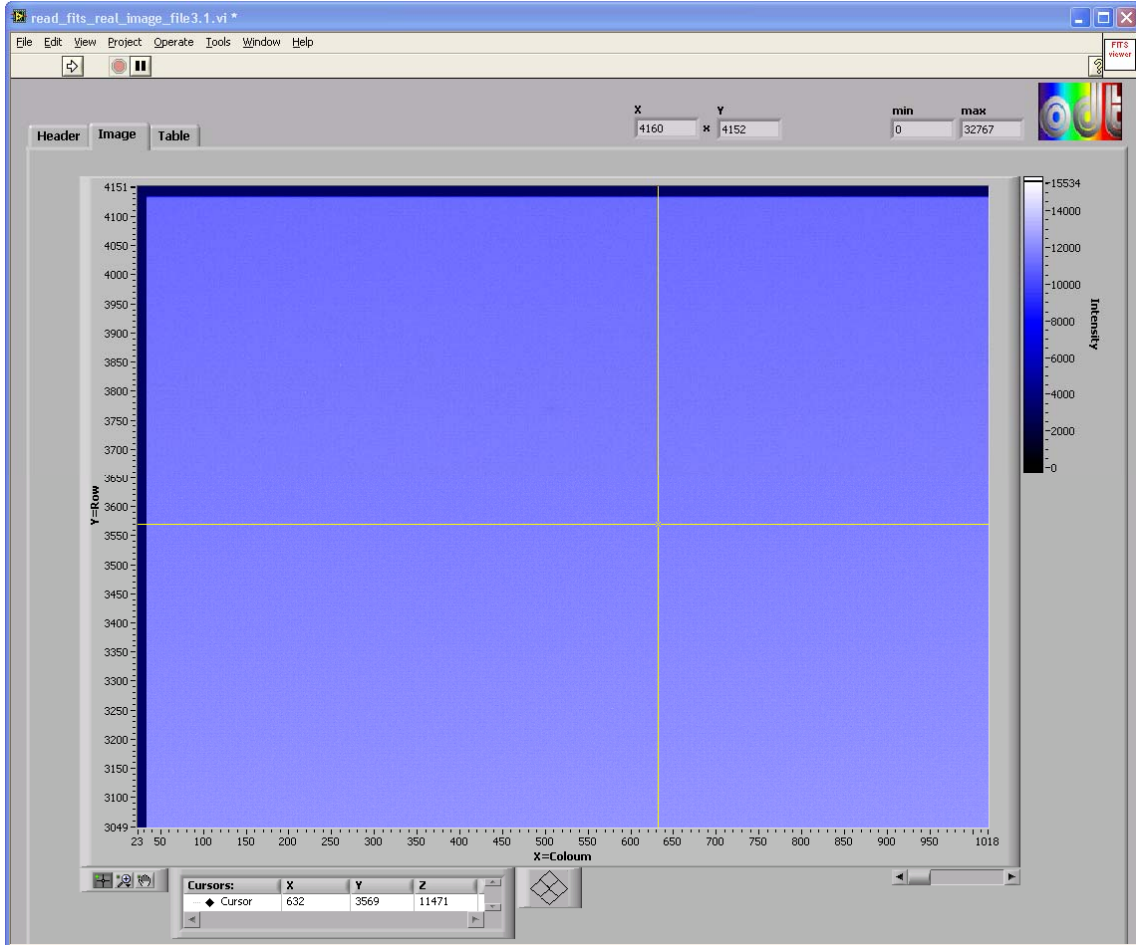


Figure 4-25: Window to display and process the FITS image

4.5.4 Automated data acquisition

Depending on the CCD controller in use, one has to choose between the two programmes *NGC_LabVIEWPRiSM_New testbench.vi* and *LabVIEWPRiSM_New testbench2.0.vi*, where the first one is the right one, if the New General Detector Controller is operated and the second one, if the FIERA system is operated. The main difference between both is the syntax that causes the controller to work. Thus the following description regards to both modules.

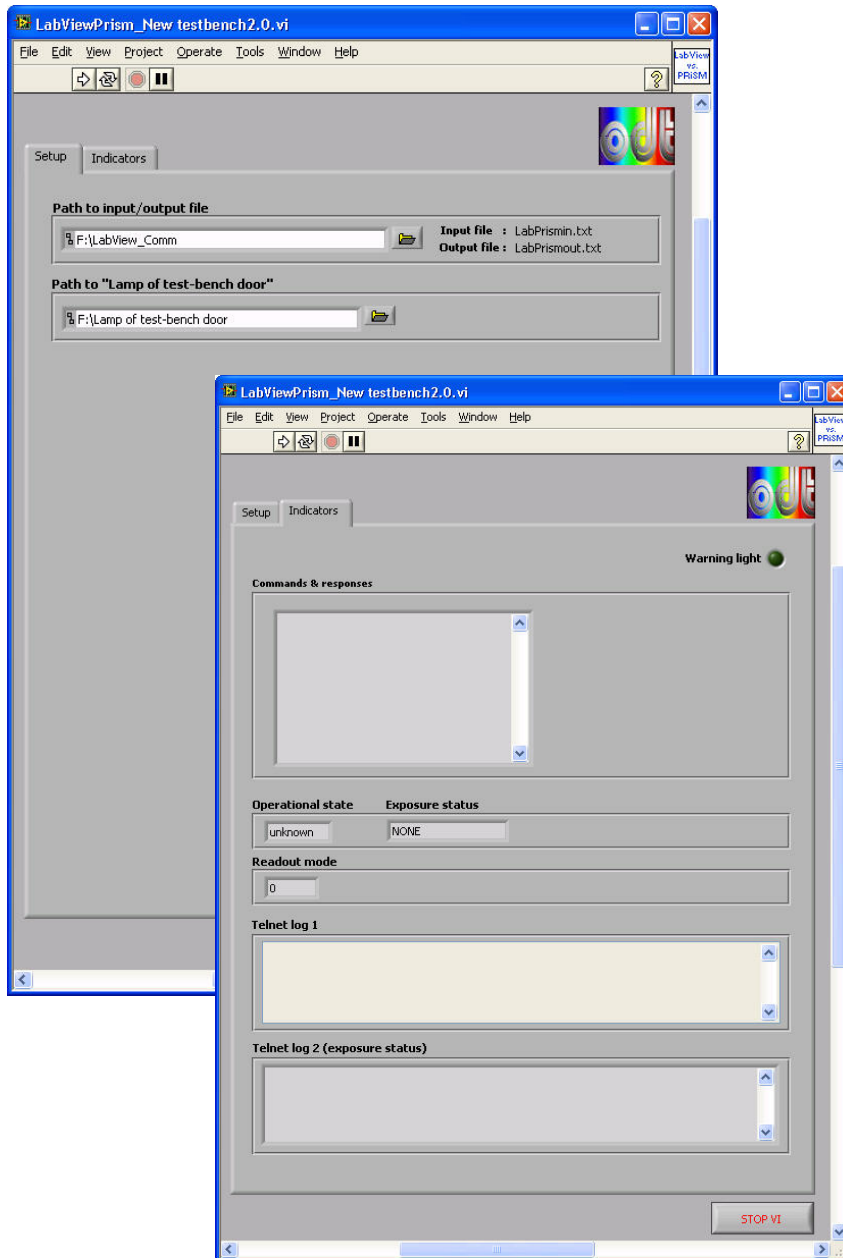


Figure 4-26: GUI of the *LabVIEWPRiSM_New testbench2.0.vi*

On page Setup in the *LabVIEWPRiSM_New testbench2.0.vi* (see 4-26) the user can specify where the input file *LabPrismin.txt* (the instructions are read from this file) and the output file *LabPrismout.txt* (the results are written into this file) are located. In addition the

directory for a further file is settable, namely the *Constant.txt* file and the *Blink.txt* file, which triggers *LabVIEW* to operate the test bench warning light (indicates that tests are in progress) placed above the entrance door.

On page *Indicators* the commands sent and received from the *PRiSM* software, the *Operational state* of the CCD controller, the *Exposure status* and the *Readout mode*, used to take the exposure, are displayed. The two telnet log windows allow to monitor the data traffic between the detector controller and the *LabVIEW* software.

After having started the *LabVIEWPRiSM_New testbench2.0.vi*, an initialization of the test bench devices is initiated. Depending on the shutter to be used (settable in the *Acquisition_Setup.vi*) either the *Prontor* shutter or the internal monochromator shutter is opened, where the other one is closed. In case the *Prontor* shutter is chosen it would be closed and the second one would be opened, to allow unhindered light throughput to the point of the *Prontor* shutter housing. In a further step the status of the test bench lamp is queried and a dialog box appears, if it is turned off. It seems to be a trivial or even questionable step, but experience has shown that it is most useful. The message can be ignored if only dark exposures are intended to be taken.



Figure 4-27: Appearing dialog box if the test bench halogen lamp is turned off

Afterwards the VI opens a telnet connection to the embedded computer of the NGC system and logs in by applying the login parameters, specified in the *DeviceDriver_Setup.vi*. The operational state of the system is read and displayed on the front panel of the application software.

The following example intends to demonstrate the proceedings, when the *PRiSM* software requests a flat field exposure of 1 second exposure time. Assuming that wavelength, bandwidth and optical density has already been set the following steps take place.

At first the *LabPrismin.txt* file is created by the *PRiSM* software containing the command to set the read out mode, or rather the clock mode (CCDF CL 10). The *LabVIEW* software reads and deletes the file, interprets the command, and temporarily saves this setting. A new *LabPrismin.txt* file created by *PRiSM* contains the command to take a flat field image of one second exposure time (CCDF FF 1000). From this point on the *LabVIEW* software carries out the requested actions. At first the lamp controller of the QTH lamp is queried, if the lamp is still turned on. The procedure is aborted and a dialog box appears in case it is turned off (lamp is most likely broken). Otherwise the *KE 2100* electrometer is triggered to read the voltage at the attached photodiode to make sure the room light level is below the preset limit (settable in the *Acquisition_Setup.vi*). There are two possible reasons for an increased room light level, either the light is turned on or the test bench door is opened. The software automatically turns off the room light and brings up a window in case the door is opened. If the door is closed and the light level is ok, the necessary commands are finally sent to the embedded computer of the CCD controller. The CCD controller FIERA (CCDF) is requested to set the clock mode (CL) to 10 and to take a flat field exposure (FF) of 1000ms exposure time by sending the appropriate commands via telnet connection (see figure 4-28 for the commands sent).

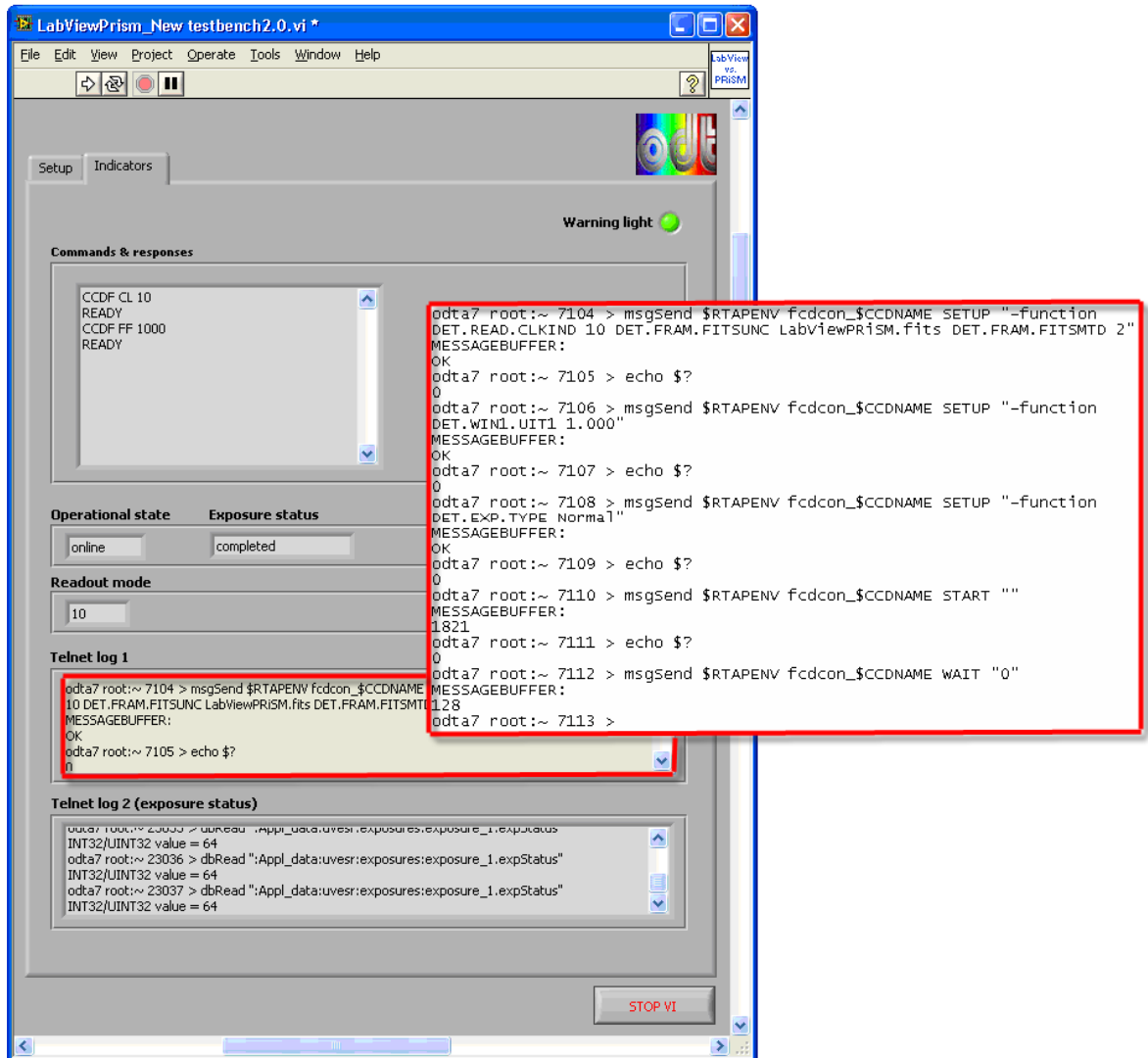


Figure 4-28: Commands sent and responses received via telnet connection, when a light exposure is taken

After the image named *LabViewPRiSM.fits* is saved in the specified directory (defined in the *Acquisition_Setup.vi*) the image header is filled with necessary information like CCD temperature and the pressure predominating in the CCD head, which is read from PULPO. Finally the *LabPrismout.txt* file is created containing the information, that the required image is available. *PRiSM* accesses the new image, performs the necessary calculations and image processing and saves it lossless compressed (CPA file format) in the CCD type

specific directory model as shown in figure 4-29. Depending on the read out mode (read out speed), the whole procedure takes around one or two minutes.

4.5.5 Data reduction and results

All the images acquired during the characterization process, the test scripts used, notes and other necessary data like specifications and the manufacturers test result for the respective detector are stored in a general CCD directory model (see figure 4-29). A painstaking storage of the raw data is absolutely essential to be able to resort to it in the future.

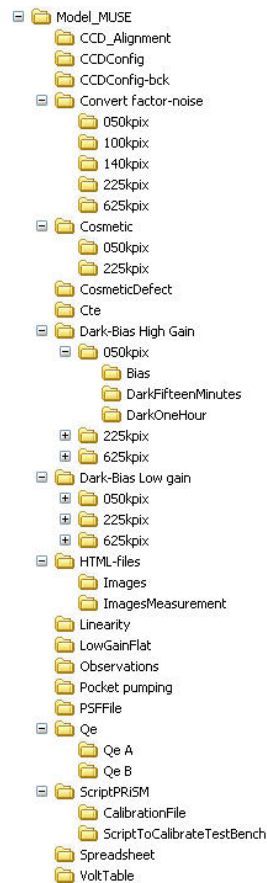


Figure 4-29: Directory model, where the raw data, the results of the characterization and all other necessary data concerning the detector are stored

The results of quantum efficiency, photo response non uniformity (PRNU), readout noise (RON), linearity, dark current, charge transfer efficiency (CTE) and cosmetic defects are summarized in an *Excel* file, which gathers the necessary data and summarizes and visualizes the outcome in a structured and well-arranged way, using the visual basic script function in *Excel*. See the annex (figure III-1, III-2, III-3 and III-4) for the template of a detector test report. The blue fields in the template are filled with data, which is read from several directories in the directory model.

5 Measurements and results

5.1 Wavelength accuracy

In order to verify, if the wavelength accuracy of the monochromator still meets the requirements after having replaced the standard slit assembly by the motorized slit assembly a random test is performed before the final assembly of the light source (including imaging optic) and the monochromator. The intention is to detect strong emission lines of a spectral lamp placed at the input, by measuring the photocurrent of the diode, attached to the integrating sphere, at the monochromator output.

Therefore an *ORIEL* low pressure mercury penlight (model 6036 and appropriate power supply model 6048) is placed at the input slit, as shown in figure 5-1, and the monochromator bandwidth is set up to its minimum at 0.5nm. Furthermore the room light is turned off and an aluminium bracket is placed behind the lamp to reduce stray light and to avoid intervisibility.

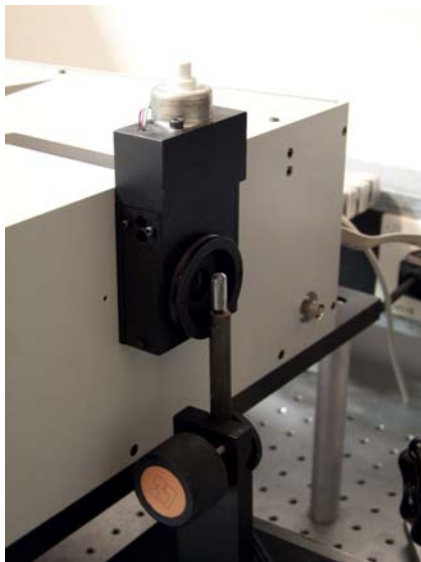


Figure 5-1: *ORIEL* low pressure mercury lamp placed at the input port of the *MSH 301*

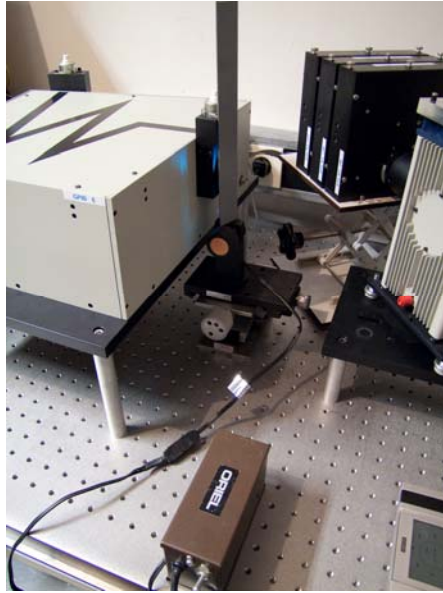


Figure 5-2: *Oriel* low pressure Hg lamp and power supply

The measurements are done interactively from a remote PC, using the standalone *LabVIEW* software modules for the monochromator and the *Keithley* 6514 electrometer. The smallest possible step size is chosen to pace up and down the critical sections of the wavelength range, where the photocurrent sharply increases (see figures 5-3, 5-4 and 5-5). According to the mercury lamp manual (and the National Institute of Standards and Technology [6]), strong emission lines can be found amongst others at 435.834nm and 546.074nm and a weak line at 1013.976nm. These three lines are chosen to be able to make a statement about the accuracy of the monochromator in the wavelength range of interest.

The yellow curve corresponds to the measurements done in positive direction and the turquoise curve corresponds to the reverse measurements. The blue, green and red line in the figures 5-3, 5-4 and 5-5 demonstrate the wavelength of the expected intensity peak, according to the emission lines of mercury.

The outcome of the evaluation of the emission line in the UV part of the spectrum is a deviation of 0.086nm in positive direction, which approximately corresponds to the minimum steps size limit (0.08nm) of the MSH 301.

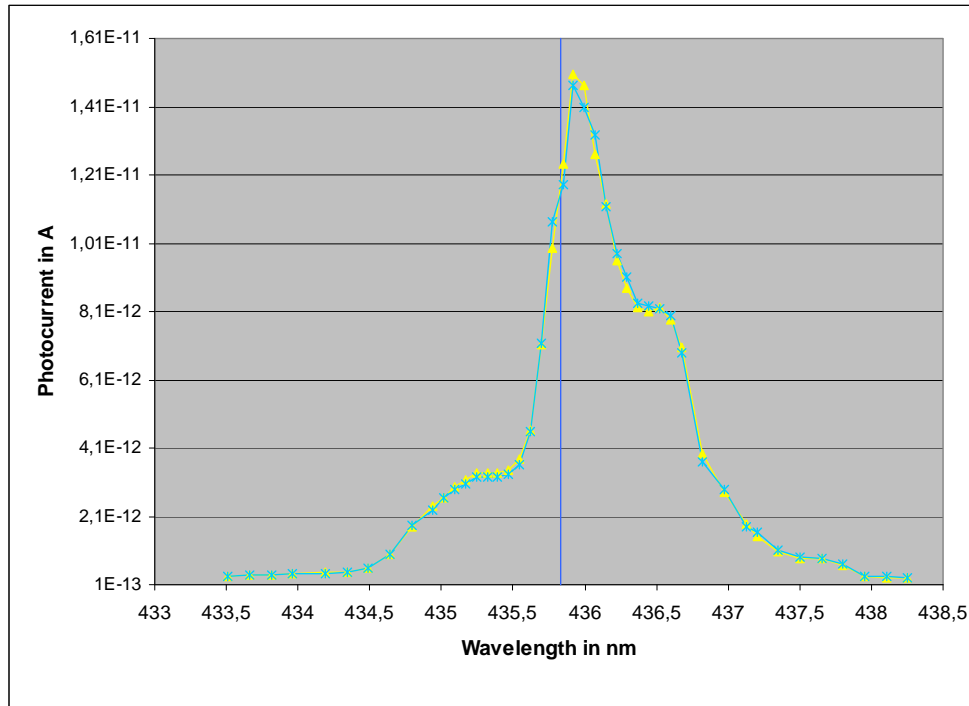


Figure 5-3: Photocurrent in A measured in the integrating sphere versus monochromator wavelength in nm and expected intensity peak at 435.834nm (blue line)

A deviation of -0.123nm is observed between the measured value and the expected value of 546.074nm. The largest aberration is obtained at the third emission line and amounts to -0.677nm.

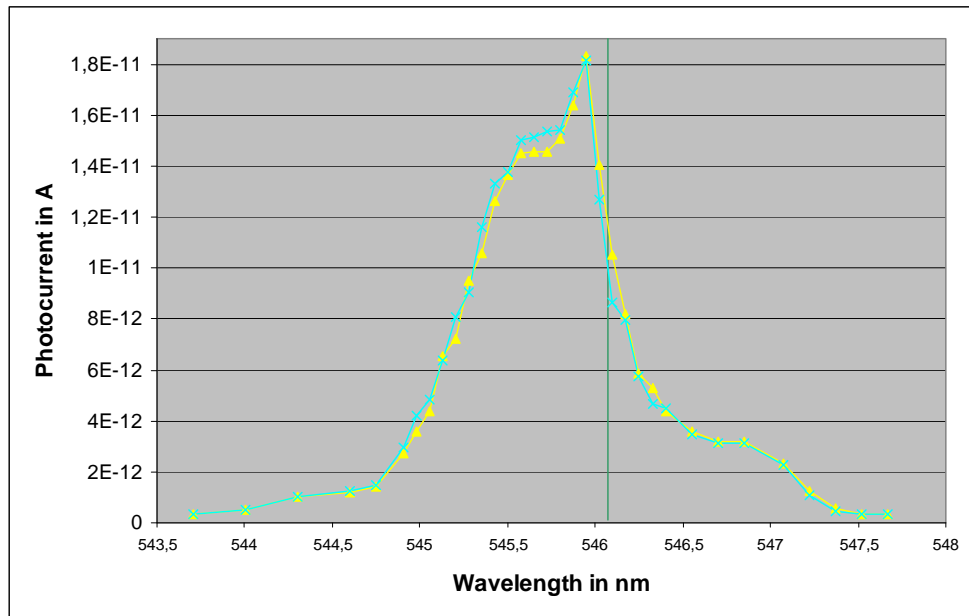


Figure 5-4: Photocurrent in A measured in the integrating sphere versus monochromator wavelength in nm and expected intensity peak at 546.074nm (green line)

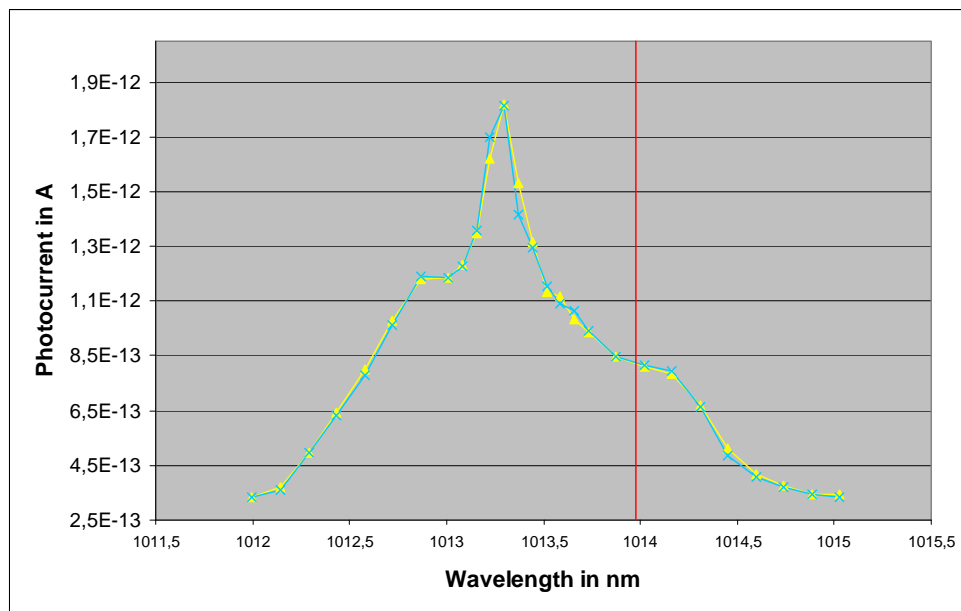


Figure 5-5: Photocurrent in A measured in the integrating sphere versus monochromator wavelength in nm and expected intensity peak at 1013.976nm (red line)

All the obtained values for the deviation of the wavelength adjustments are well inside the specifications of $\pm 1\text{nm}$. Therefore there is no need to perform a wavelength calibration of the *MSH 301*.

6 Discussion

6.1 Light performance

It is obvious that the ND-filters are not the only components in the light path that have an influence on the intensity of light reaching the detector, but it is not necessary to accurately adjust the intensity level. The transmittance of the coloured glass filters is limited and the monochromator and the integrating sphere reduce the light intensity as well. The light performance provided by the existing configuration is sufficient for the tests to be done. There are possibilities to tune the system but the necessary arrangements require new or at least modified components to be reassembled and the additional benefit remains limited. As mentioned the acceptance angle of the monochromator is not completely filled as it is necessary to achieve best efficiency. Considering the lamp housing and condenser remain the same, this could be achieved by a new lens with a focal length of 125mm, which is available and easy to replace. But the replacement would only make sense in case the filter wheels are removed from this part of the light path, because firstly the length of the wheels along the optical axis is larger than the focal length of the lens and secondly the aperture of the first filter holder would again reduce the opening ratio and stop down the light beam. In this case one has to think about where to place the filter wheels. If they are placed at the output port of the monochromator, the amount of light that reaches the integrating sphere would again decrease due to the a limited opening angle by the filter holder. Furthermore the light tight zone will minimize to an unacceptable small size, because the XYZ linear stage is intended to be placed there to perform the PSF measurements.

6.2 Additional shutter

The internal monochromator shutter is not suitable for the number of open-close procedures that are foreseen. For example during a quantum efficiency measurement, which takes about two hours to complete, the shutter is operated around 200 times, because quite often

an exposures is taken twice until integration time and optical density are adjusted in the way that the flat field exposures, taken at different wavelengths, have approximately the same light level. Moreover the photocurrent has to be measured at each wavelength of interest and therefore the shutter needs to be opened once again, in case the monochromator shutter is used. Experience has shown that these shutters break after a short period of time, they remain open for some reason or they simply stop working. According to the manufacturers specifications the *Prontor* magnetic shutter has a guaranteed life time of one million exposures and is designed to be incorporated into scientific cameras.

6.3 Wavelength adjustments

The monochromator could be tuned to the wavelength accuracy specification of 0.35nm, stated by the manufacturer, by calibrating the device with a spectral lamp and a photo detector, but the measured wavelength deviations are well inside the required accuracy of ± 1 nm. For this reason it is not necessary to perform a calibration.

6.4 Uniformity of illuminance

The calculated deviation of illuminance over the whole detector area is an acceptable value but needs to be verified by measuring. An imaginable measurement setup is a photodiode mounted onto the XYZ linear stage as close as possible to the chip position. Then the light intensity could be measured at predefined positions of a raster, which covers the area of the detector.

7 Conclusion

The test assembly provides a diffuse, uniform and monochromatic illumination of 4k x 4k pixel detectors with up to 100mm diameter mainly in the visible wavelength range. Detectors can be illuminated at adjustable intensity, bandwidth and wavelength where all necessary devices can be operated interactively or in fully automated procedures from a remote location. The CCD cryostats can be exchanged in few steps without touching critical components of the test setup. Except few custom-made parts, standard lab components were used. This provides the opportunity for modifications and upgrades in the future. The functionality of the software can easily be enlarged by editing the existing modules or embedding new pieces of software. Both available CCD controllers are supported by the software.

PSF experiments are virtually possible, but the necessary hardware is currently not installed, because it is used at another measurement setup.

Applicable documents

- [1] REISS, Roland: MUSE IDS Detectors Technical Specification, VLT-SPE-ESO-14679-4377. Garching bei München, European Southern Observatory (April 2008)

- [2] AMICO, P., BÖHM, T. In Beletic, J. and Amico, P.: Optical Detectors for Astronomy. Vol.1, Kluwer Academic Publishers (1998)

- [3] CAVADORE, C., Christen, F., and Darbon, S.: New Testbench Software User's Manual. Garching bei München, European Southern Observatory (2002)

- [4] KINGSLAKE, Rudolf: Applied Optics and Optical Engineering. Vol.2, Academic Press Inc. (1965)

- [5] MÜLLER, Eric. <emueller@eso.org>, DEIRIES, Sebastian <sdeiries@eso.org> MÜLLER E., Deiries S.: ODT Test-bench *LabVIEW* Modules User Manual, GEN-MAN-ESO-21110-0028. URL:<<http://www.eso.org/projects/odt/ODTnew/index.html>>, available on 23.06.2009

- [6] National Institute of Standards and Technology. Unknown author: Basic Atomic Spectroscopic Data - Strong Lines of Mercury (Hg). URL: <<http://physics.nist.gov/PhysRefData/Handbook/Tables/mercurytable2.htm>>, available on 23.06.2009

- [7] BALESTRA, Andrea <andrea.balestra@eso.org>, CUMANI, Claudio <ccumani@eso.org>. Balestra, A., Cumani, C.: FIERA CCD Controller Software User Manual, Doc.No. VLT-MAN-ESO-13640-1388. URL: <http://www.eso.org/projects/vlt/sw-dev/wwwdoc/JAN2006/VLT-MAN-ESO-13640-1388/Output/fro_.html>, available on 23.06.2009

- [8] BALESTRA, Andrea <andrea.balestra@eso.org>, CUMANI, Claudio <ccumani@eso.org>. Balestra, A., Cumani, C.: Next Generation detector Controller Optical DCS - User Manual, Doc.No. VLT-MAN-ESO-13660-4086. URL: <<http://www.eso.org/projects/odt/ODTnew/index.html>>, available on 23.06.2009
- [9] GEIMER, C. <cgeimer@eso.org>, CUMANI, Claudio <ccumani@eso.org>. Geimer, C., Cumani, C.: PULPO-2 manual, VLT-TRE-ESO-13630-3490. URL: <http://www.eso.org/tecarch/Documents/VLT/13000_optical_instruments/13600_vlt_scientific_CCD_system/13630-pulpo/VLT-TRE-ESO-13630-3490-2.0.pdf>, available on 23.06.2009
- [10] WICHER Carola. <Carola.Wicher@fh-jena.de>. Wicher C. Hinweise zur Gestaltung von Bachelorarbeiten an der Fachhochschule Jena im Studiengang Augenoptik. URL: <<http://www.fh-jena.de/~wicher>>, available on 23.06.2009
- [11] Keithley. <info@Keithley.com>. Unknown author: Model 6514 System Electrometer Instruction Manual. URL: <<http://www.Keithley.com/products/locurrhiresist/electrometers/?mn=6514>> and <<http://www.Keithley.com/data?asset=52529>>, available on 23.06.2009
- [12] Keithley. <info@Keithley.com>. Unknown author: Model 2100 6 1/2-Digit Resolution Digital Multimeter User's Manual. URL: <<http://www.Keithley.com/products/dmm/dmms/?mn=2100120>> and <<http://www.Keithley.com/data?asset=50760>>, available on 23.06.2009
- [13] Newport. <oriel.sales@newport.com>. Unknown author: Motorized Filter Wheel System Model 74041 User Manual. URL: <<http://search.newport.com/?sku=74041>>, available on 23.06.2009

- [14] Newport. <germany@newport.com>. Unknown author: 1/4 M Monochromator Model MSH 301 User Manual. URL: <http://www.LOT-ORIEL.com/site/site_down/ms_101301_fren.pdf> and <<http://search.newport.com/?sku=74100>>, available on 23.06.2009
- [15] Newport. <oriel.sales@newport.com>. Unknown author: 300W Radiometric Power Supply Model 69931 User Manual. URL: <<http://search.newport.com/?sku=69931>>, available on 23.06.2009
- [16] Newport. <germany@newport.com>. Unknown author: ESP300 Motion Controller/Driver User's Manual. URL: <<http://search.newport.com/?sku=ESP300-111112>>, available on 23.06.2009
- [17] Newport. <oriel.sales@newport.com>. Unknown author: Unknown title. URL:<<http://www.newport.com/images/webclickthru-GR/images/2282.gif>>, available on 23.06.2009
- [18] *Velleman Inc.*. <export@Velleman Inc..be>. Unknown author: Introduction to the DLL for the USB experiment interface board K8055. URL: <http://www.Velleman Inc..be/downloads/0/user/usermanual_k8055_dll_uk.pdf>, available on 23.06.2009
- [19] *Velleman Inc.*. <export@Velleman Inc..be>. Unknown author: USB Experiment interface board K8055. URL: <http://www.VellemanInc.be/downloads/0/illustrated/illustrated_assembly_manual_k8055_uk_rev3.pdf>, available on 23.06.2009
- [20] LOT-ORIEL. <mentges@LOT-ORIEL.de>. Unknown author: Standard-Ulbrichtkugeln, BaSO₄. URL: <http://www.LOT-ORIEL.com/site/site_down/ul_baso4_dede.pdf>, available on 23.06.2009

- [21] RUPPRECHT, G. <grupprec@eso.org>. Rupprecht, G.: CCD Characterization Procedure, Doc.No. VLT-PRO-ESO-13600-4686.
URL: <http://www.eso.org/tecarch/Documents/VLT/13000_optical_instruments/13600_vlt_scientific_CCD_system/VLT-PRO-ESO-13600-4686_i1.pdf>, available on 23.06.2009
- [22] CHRISTEN, F (2003). Characterization of the OmegaCAM CCDs with the ESO test bench. URL: <<http://www.eso.org/projects/odt/ODTnew/index.html>>, available on 23.06.2009
- [23] PRONTOR. <robra@prontor.de>. Unknown author: PRONTOR MAGNETIC SHUTTER E/64 - Specifications. URL:<http://www.schneideroptics.com/pdfs/industrial/Prontor_magnetic_shutter_E64.pdf>, available on 23.06.2009
- [24] SCHRÖDER, Gottfried: Technische Optik. Vol.7, Vogel, Würzburg (1990)
- [25] Newport. <oriel.sales@newport.com>. Unknown author: Unknown title.
URL:<<http://www.newport.com/images/webclickthru-EN/images/1216.gif>>, available on 23.06.2009

Numbering	Title	Page
Figure 3-1:	The first science grade CCD (named CERES) for MUSE	6
Figure 4-1:	Time delayed integration (TDI) image of a 4096x2048 pixel detector	9
Figure 4-2:	Polychromatic light diffracted by a grating [14]	13
Figure 4-3:	The new CCD test bench	15
Figure 4-4:	CAD model of the test bench components with an impact on the light path including their controllers	18
Figure 4-5:	Custom-made components at the test bench	19
Figure 4-6:	Magnified imaging of the filament onto the monochromator input slit by means of the condenser optic (Filters not drawn) [17]	21
Figure 4-7:	The asymmetrical in-plane Czerny-Turner optical configuration of the <i>Newport MSH 301</i> monochromator [25]	22
Figure 4-8:	The test bench light path	23
Figure 4-9:	Oblique illuminance of the detector (on the right) from a self-luminous disk (output port of the integrating sphere) [4]	24
Figure 4-10:	Software hierarchy	26
Figure 4-11:	The front panel of the <i>PowerSupply_standalone.vi</i> (on the left) and the dialog box to set the current and power level.	30
Figure 4-12:	Front panel of the <i>Filter_wheel_standalone.vi</i>	31
Figure 4-13:	Front panel of the <i>MSH 301_standalone2.1.vi</i> , with page <i>Basic</i> located on the left and page <i>Expert</i> (wrong settings can cause malfunction of the device) on the right	32
Figure 4-14:	Front panel of the <i>Keythley_6514_standalone2.0.vi</i>	33
Figure 4-15:	Front panel of the <i>Keithley 2100 Series Read Single.vi</i>	34
Figure 4-16:	The user interface of the <i>ESP300_standalone.vi</i> (on the left) and the window to set axis velocity, acceleration and deceleration	35
Figure 4-17:	Page <i>Table</i> of the front panel of the <i>Pulpo1_standalone2.0.vi</i>	36

Table of figures

Figure 4-18:	Page <i>Controls</i> of the front panel of the <i>Pulpo1_standalone2.0.vi</i>	37
Figure 4-19:	Page <i>Chart</i> of the front panel of the <i>Pulpo1_standalone2.0.vi</i>	37
Figure 4-20:	Page <i>Controls</i> of the <i>JUMO_standalone2.0.vi</i> front panel	38
Figure 4-21:	Page <i>JUMO 1</i> of the <i>JUMO_standalone2.0.vi</i> front panel which displays the values of the sensors connected to the first <i>JUMO</i>	39
Figure 4-22:	Front panel of the <i>USB Interface Board_standalone2.0.vi</i>	40
Figure 4-23:	Page <i>Setup</i> of the <i>FIERA_standalone.vi</i>	41
Figure 4-24:	Page <i>Indicators</i> of the <i>FIERA_standalone.vi</i>	42
Figure 4-25:	Window to display and process the FITS image	43
Figure 4-26:	GUI of the <i>LabVIEWPRiSM_New testbench2.0.vi</i>	44
Figure 4-27:	Appearing dialog box if the test bench halogen lamp is turned off	45
Figure 4-28:	Commands sent and responses received via telnet connection, when a light exposure is taken	47
Figure 4-29:	Directory model, where the raw data, the results of the characterization and all other necessary data concerning the detector are stored	48
Figure 5-1:	<i>ORIEL</i> low pressure mercury lamp placed at the input port of the <i>MSH 301</i>	50
Figure 5-2:	<i>ORIEL</i> low pressure Hg lamp and power supply	51
Figure 5-3:	Photocurrent in A measured in the integrating sphere versus monochromator wavelength in nm and expected intensity peak at 435.834nm (blue line)	52
Figure 5-4:	Photocurrent in A measured in the integrating sphere versus monochromator wavelength in nm and expected intensity peak at 546.074nm (green line)	53
Figure 5-5:	Photocurrent in A measured in the integrating sphere versus monochromator wavelength in nm and expected intensity peak at 1013.976nm (red line)	53

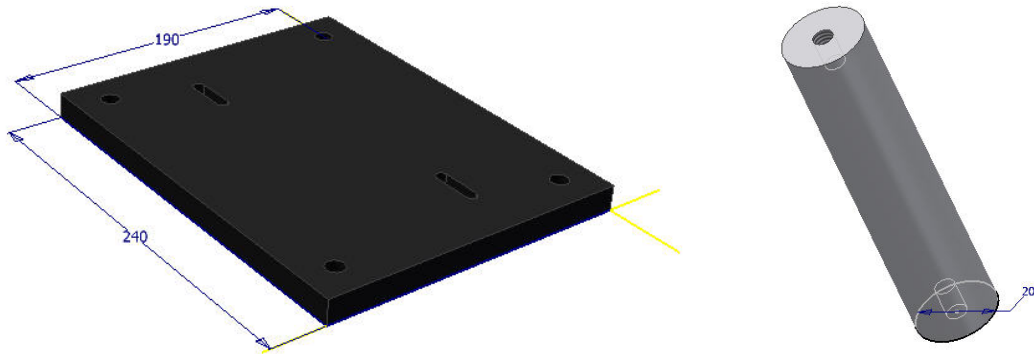


Figure I-1: CAD model of plate and rod (all in all four rods) for uplifting the lamp housing onto the optical axis. (Part I in figure 4-5)

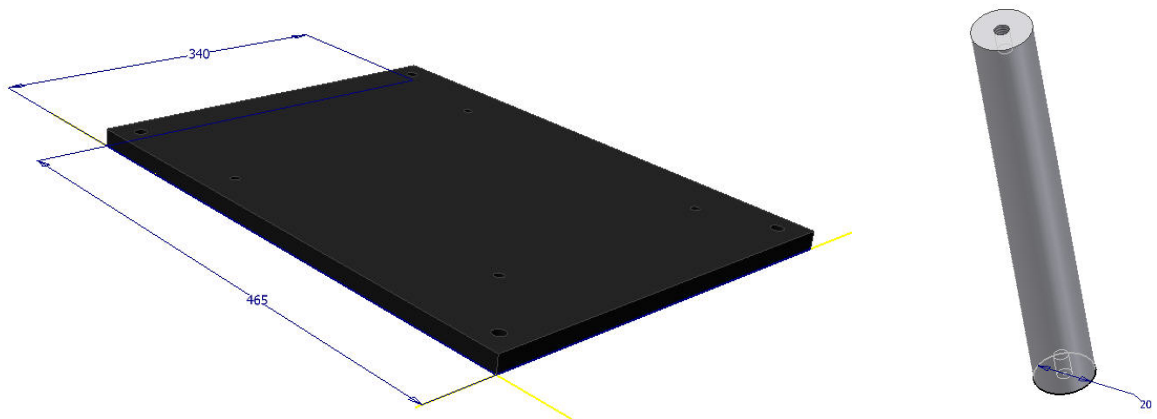


Figure I-2: CAD model of plate and rod (all in all four rods) for uplifting the monochromator onto the optical axis. (Part I in figure 4-5)

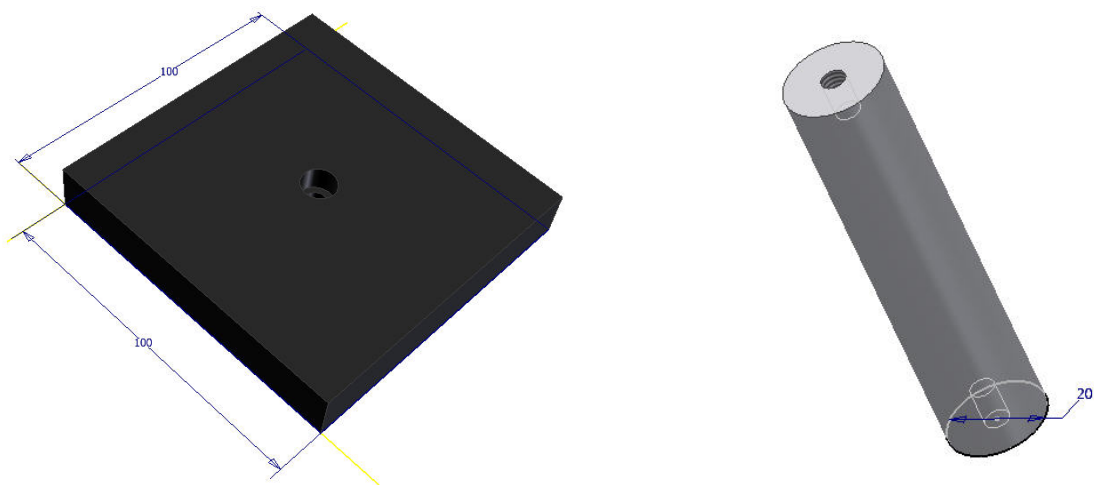


Figure I-3: CAD model of plate and rod for uplifting the integrating sphere onto the optical axis. (Part I in figure 4-5)

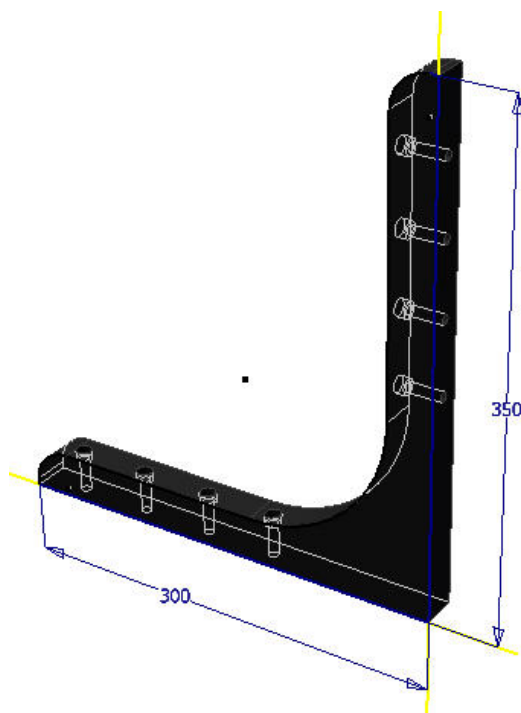


Figure I-4: CAD model of the bracket (all in all two) that holds the plate (see figure I-5) in a rectangular position to the optical table. (Part IX in figure 4-5)

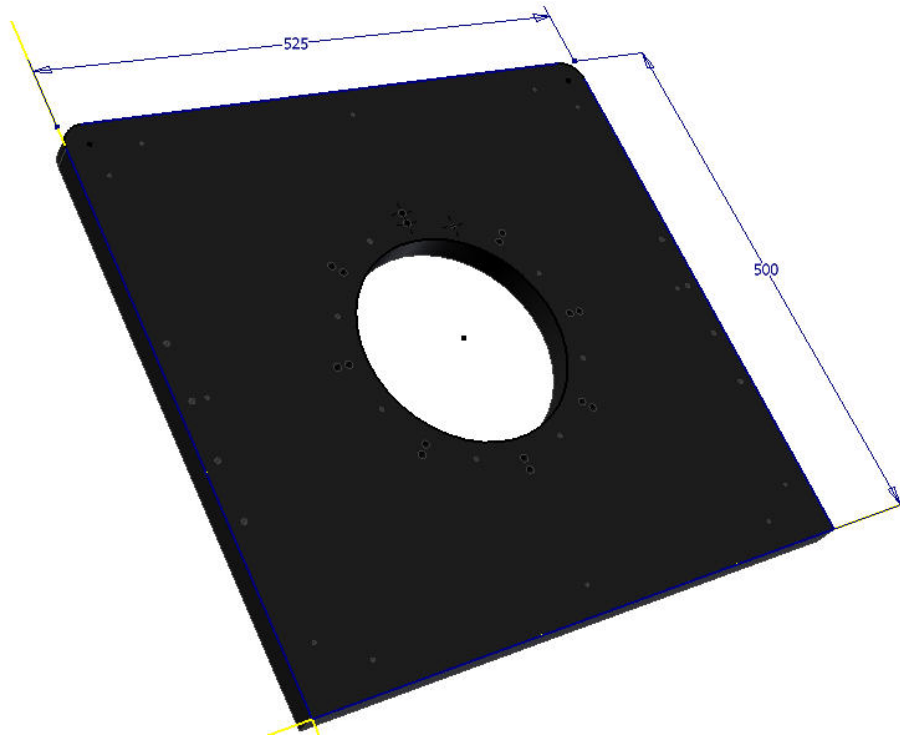


Figure I-5: CAD model of plate for uplifting the CCD cryostat onto the optical axis. (Part VIII in figure 4-5)

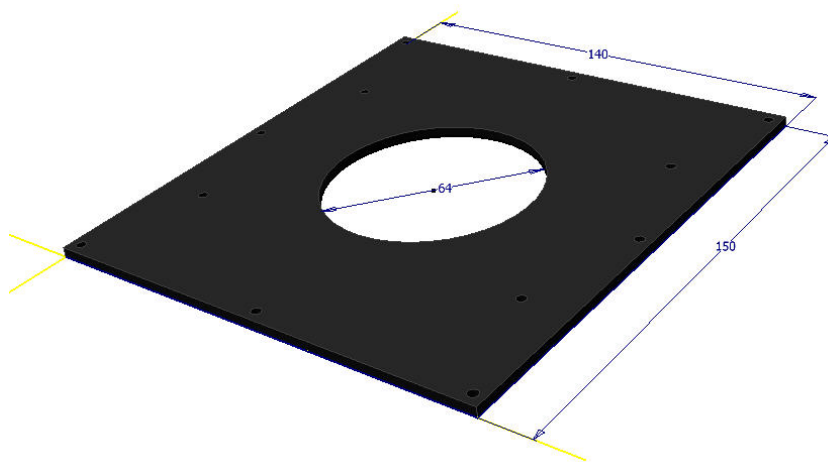


Figure I-6: CAD model of the cover of the shutter housing. The shutter is mounted to this cover before cover and housing (see figure I-7) are assembled. (Part V in figure 4-5)

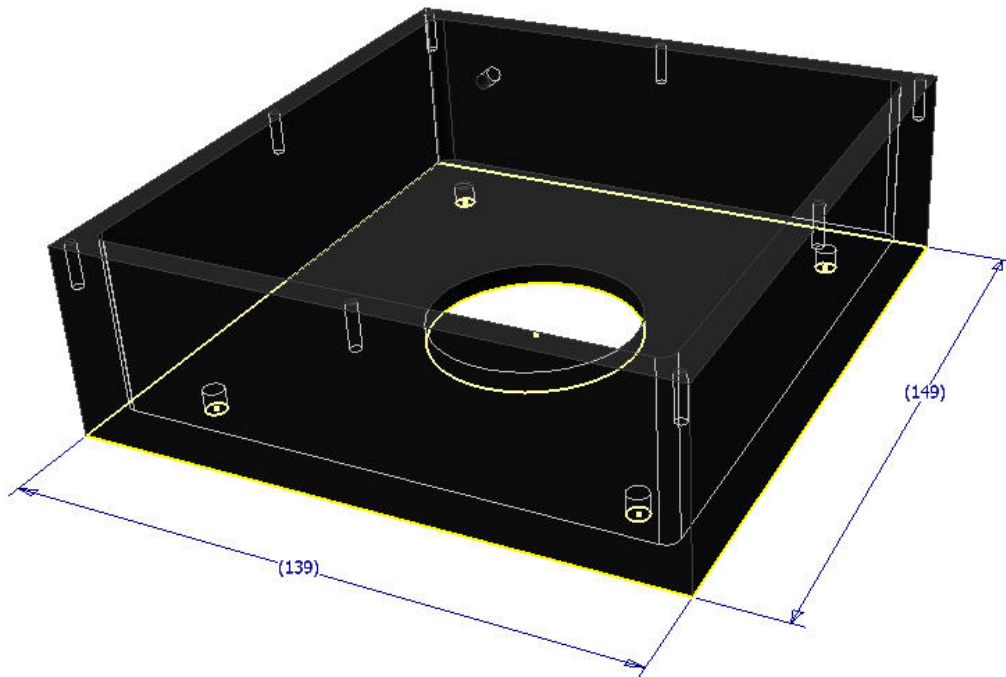


Figure I-7: CAD model of the shutter housing. (Part V in figure 4-5)

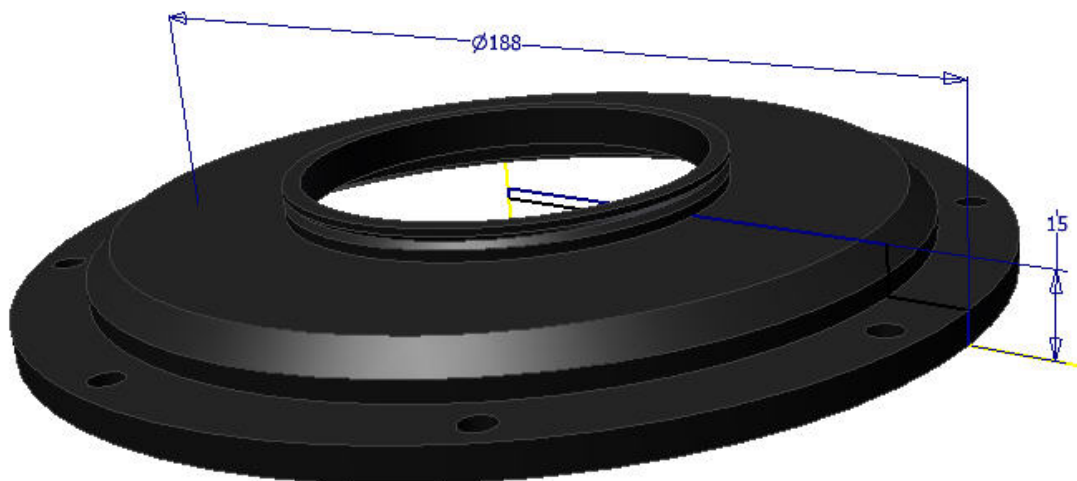


Figure I-8: CAD model of the flange where the image projector is attached to. It is then mounted onto the CCD head. (Part VII in figure 4-5)

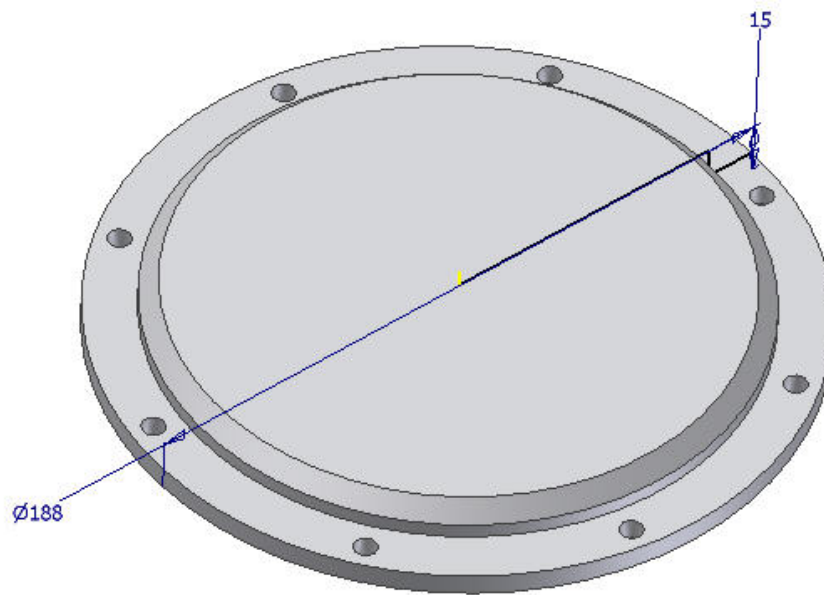


Figure I-9: CAD model of the metallic cover which is attached to the CCD head when dark exposures are taken. (Part VI in figure 4-5)



Figure I-10: CAD model of the two rings that keep the photodiode attached to the integrating sphere. (Part IV in figure 4-5)



Figure I-11: CAD model of the flange between integrating sphere and monochromator. (Part II in figure 4-5)

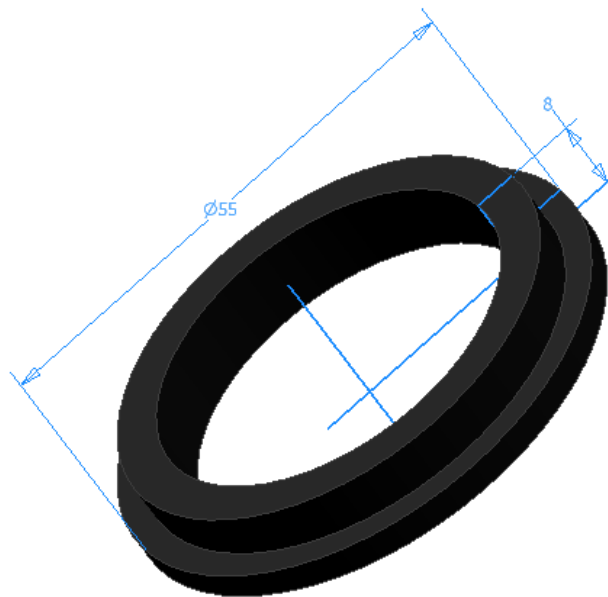


Figure I-12: CAD model of the ring which mounted to the output port of the integrating sphere. It allows to attach an opaque tissue which connects the sphere and the wooden light-tight box. (Part III in figure 4-5)

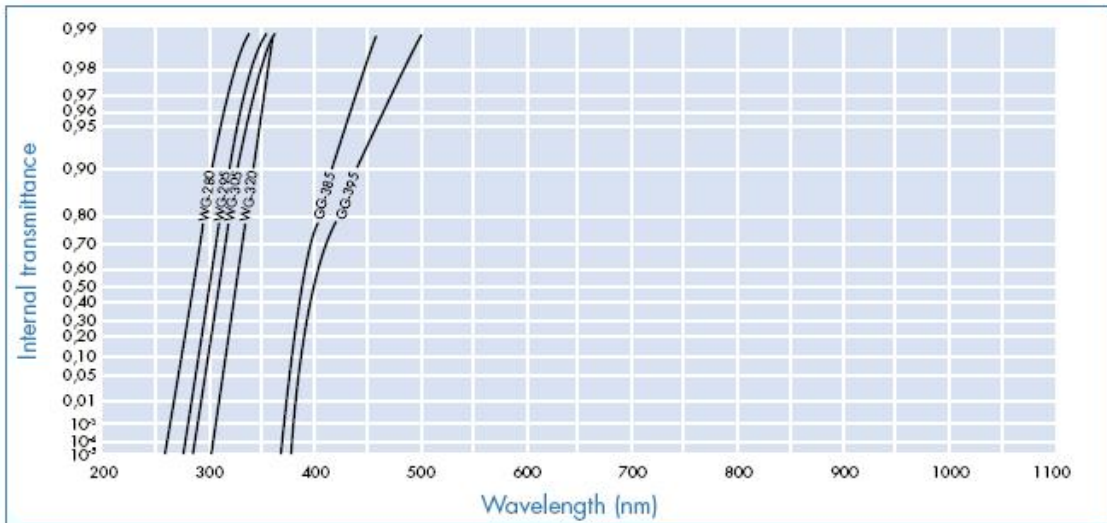


Figure II-1: Internal transmittance versus wavelength of order sorting filter 305FG01-25 (equates to type of filter WG-305)

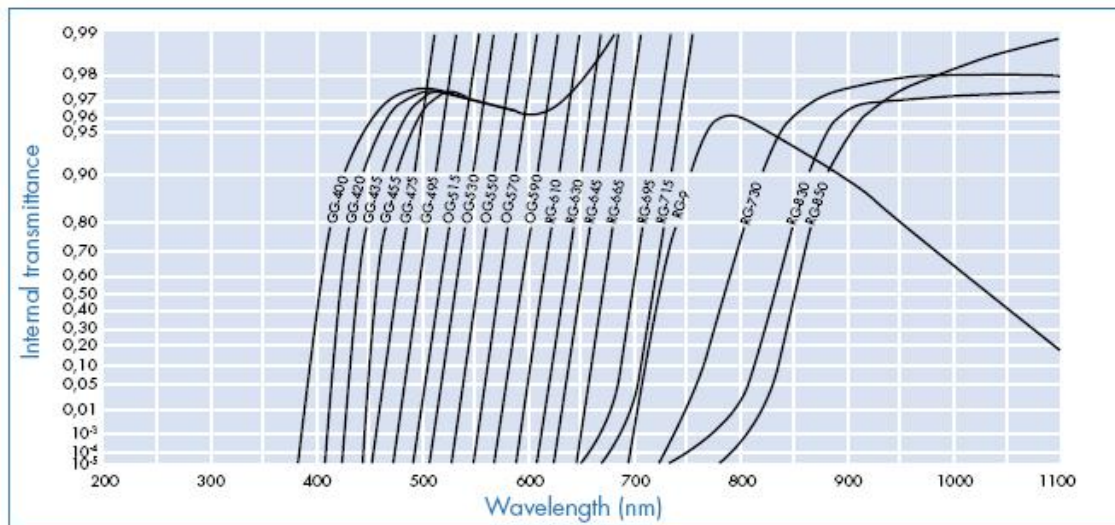


Figure II-2: Internal transmittance versus wavelength of order sorting filter 550FG05-25 (equates to type of filter OG-550)

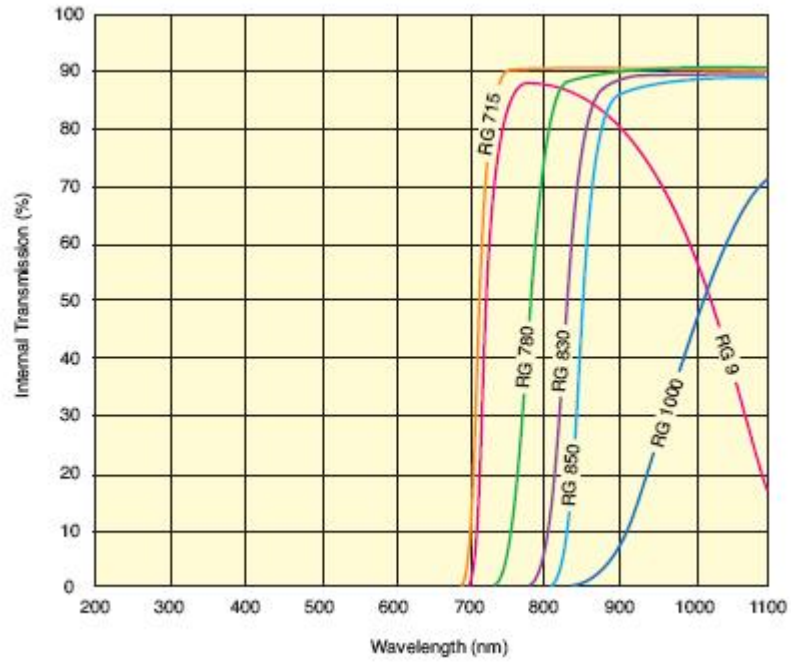


Figure II-3: Internal transmittance versus wavelength of order sorting filter FSR-RG1000 (equates to type of filter RG-1000)

Transmission in %	Type of glass	Thickness in mm
70.79	NG11	1.2
70.79	NG11	1.2
50.11	NG11	2.5
25.11	NG4	1.2
10.00	NG4	2.0
5.01	NG4	2.5
2.51	NG9	1.1
0.5	NG9	1.6
0.1	NG9	2.1
0.025	NG9	2.5

Figure II-4: List of the ND-filters mounted in the filter wheels.

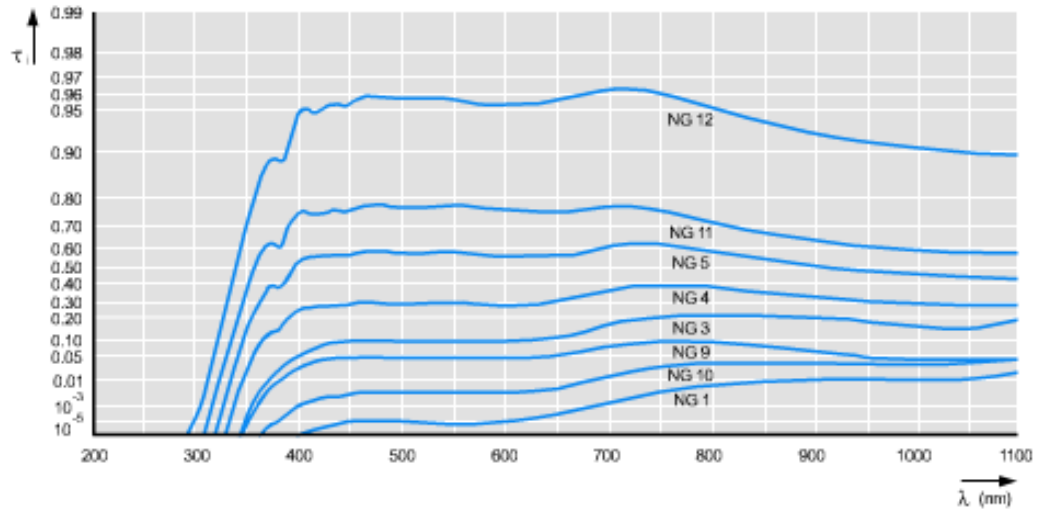


Figure II-5: Transmittance of *SCHOTT* neutral density filters of type NG4, NG9 and NG11

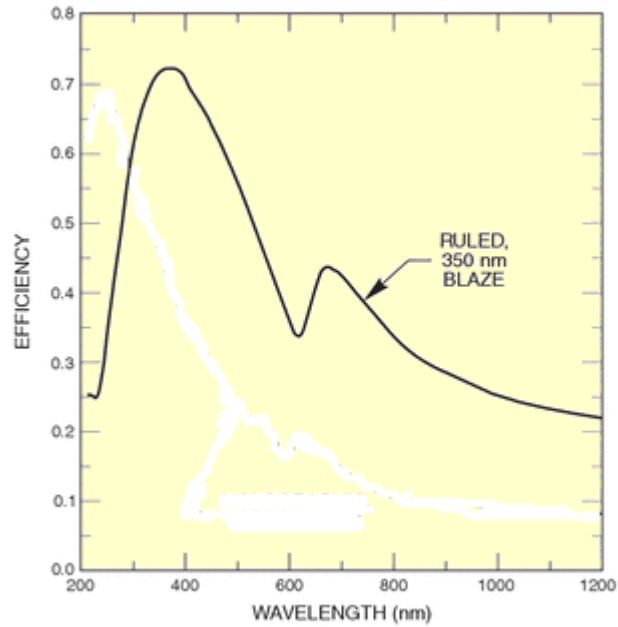


Figure II-6: Typical efficiency of ruled gratings with 350nm blaze wavelength.

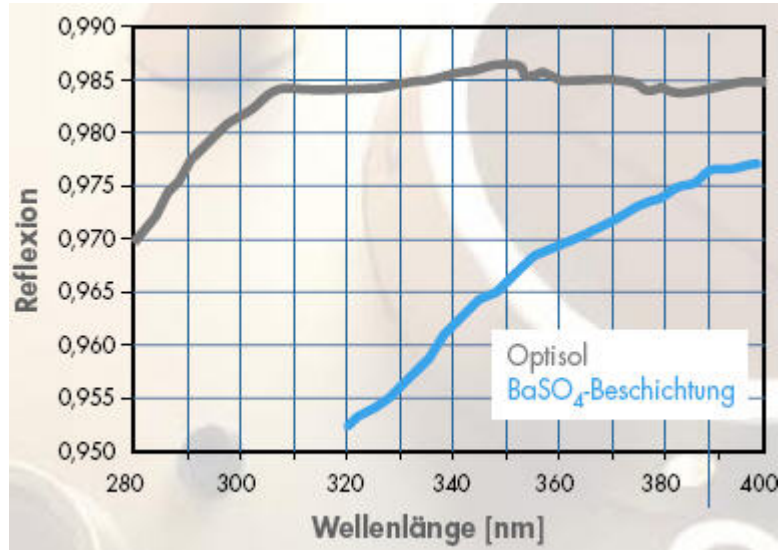


Figure II-7: Integrating sphere coating (BaSO_4) reflectance as a function of wavelength (320nm to 400nm).

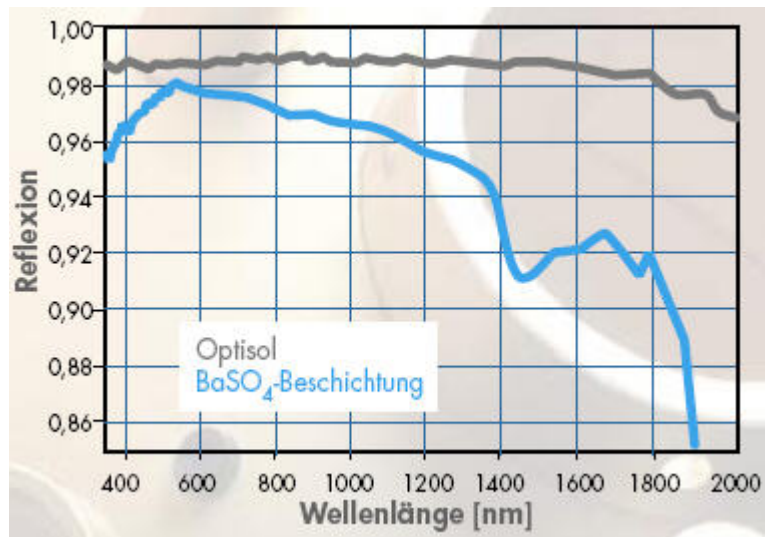


Figure II-8: Integrating sphere coating (BaSO_4) reflectance as a function of wavelength (400nm to 2000nm).

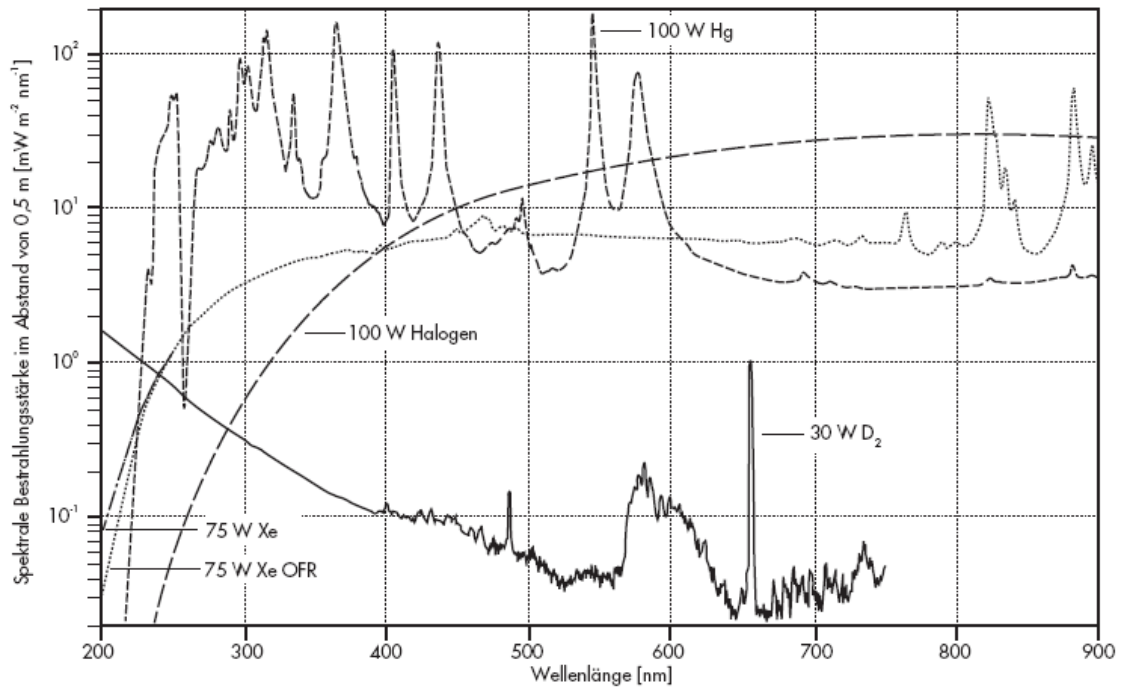


Figure II-9: Spectral irradiance of a 100 W halogen lamp in 0.5m distance

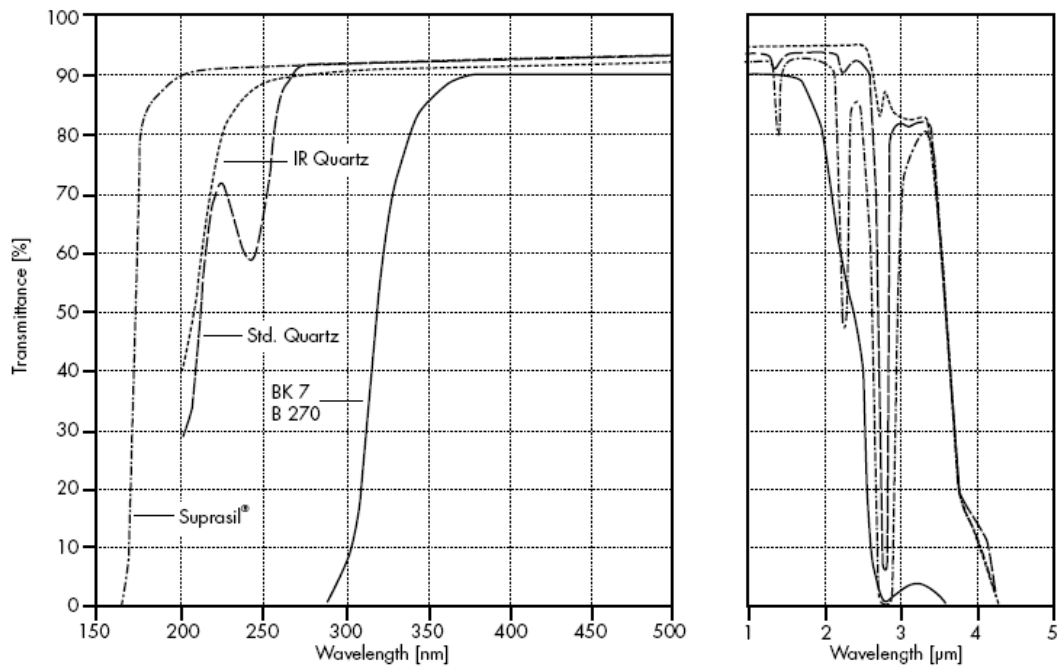


Figure II-10: Transmittance of 10mm thick standard quartz (material of lenses)

Quantum Efficiency/ Photo- Response Non- Uniformity

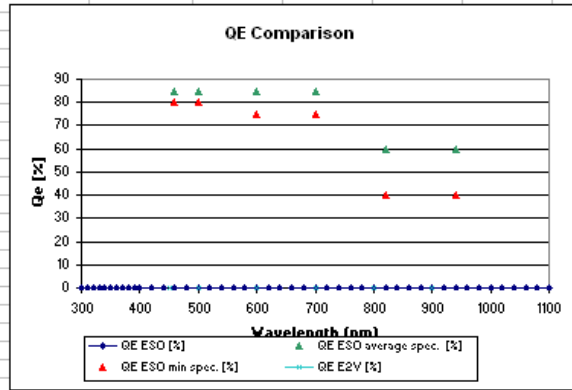


Figure 1: Comparison between the QE measured by ESO, the QE measured by E2V, ESO specification and minimum specification

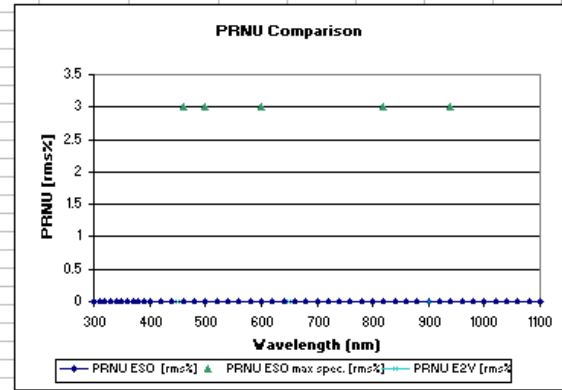


Figure 2: Comparison between the PRNU measured by ESO, the PRNU measured by E2V, ESO specification and maximum specification

Clockmode:	#TBD
Conversion Factor [e-/A]	#TBD #TBD
RMS noise [e-]	#TBD #TBD
CCD temperature [C]:	#TBD

Wavelength [nm]	ESO					Fringing	E2V	
	QE ESO [%]	PRNU ESO [rms%]	QE ESO average spec. [%]	QE ESO min spec. [%]	PRNU ESO max spec. [%]		QE E2V [%]	PRNU E2V [rms%]
300	#TBD	#TBD						
310	#TBD	#TBD						
320	#TBD	#TBD						
330	#TBD	#TBD						
340	#TBD	#TBD						
350	#TBD	#TBD						
360	#TBD	#TBD						
370	#TBD	#TBD						
380	#TBD	#TBD						
390	#TBD	#TBD						
400	#TBD	#TBD						
420	#TBD	#TBD						
440	#TBD	#TBD						
450	#TBD	#TBD					#TBD	#TBD
460	#TBD	#TBD	85	80	3			
480	#TBD	#TBD						
500	#TBD	#TBD	85	80	3		#TBD	
520	#TBD	#TBD						
540	#TBD	#TBD						
560	#TBD	#TBD						
580	#TBD	#TBD						
600	#TBD	#TBD	85	75	3		#TBD	
620	#TBD	#TBD						
640	#TBD	#TBD						
650	#TBD	#TBD						#TBD
660	#TBD	#TBD						
680	#TBD	#TBD						
700	#TBD	#TBD	85	75			#TBD	
720	#TBD	#TBD						
740	#TBD	#TBD						
760	#TBD	#TBD						
780	#TBD	#TBD						
800	#TBD	#TBD					#TBD	
820	#TBD	#TBD	60	40	3			
840	#TBD	#TBD						
860	#TBD	#TBD						
880	#TBD	#TBD						
900	#TBD	#TBD					#TBD	#TBD
920	#TBD	#TBD						
940	#TBD	#TBD	60	40	3			
960	#TBD	#TBD						
980	#TBD	#TBD						
1000	#TBD	#TBD						
1020	#TBD	#TBD						
1040	#TBD	#TBD						
1060	#TBD	#TBD						
1080	#TBD	#TBD						
1100	#TBD	#TBD						
Error	±1.5 %	±0.5 %						

#TBD is updated by macro To Be Done

Figure III-2: Page two of the template for a CCD test report

Readout Noise / Conversion Factor/ Linearity/ Charge Transfer Efficiency/ Fullwell									
Port		E		F		G		H	
		ES0	E2V	ES0	E2V	ES0	E2V	ES0	E2V
Readout Noise [rms e-] at	100 kpix/s	#TBD		#TBD		#TBD		#TBD	
Readout Noise [rms e-] at	500 kpix/s		#TBD		#TBD		#TBD		#TBD
Readout Noise [rms e-] at	50 kpix/s		#TBD		#TBD		#TBD		#TBD
Conversion Factor [e-/pix/hr] at	100 kpix/s	#TBD		#TBD		#TBD		#TBD	
Linearity Deviation (1000 -100ke-) [rms%]	100 kpix/s	#TBD							
CTE	100 kpix/s	#TBD							
Amplifier (Fullwell) [ke-]	100 kpix/s	#TBD							
Blooming (Fullwell) [ke-/pix]									

Port		Parallel		Specification		
		ES0	E2V	ES0	E2V	
Readout Noise [rms e-] at	100 kpix/s			2.5		max
Readout Noise [rms e-] at	500 kpix/s				#TBD	max
Readout Noise [rms e-] at	50 kpix/s				#TBD	max
Conversion Factor [e-/pix/hr] at	100 kpix/s			0.55		recommended
Linearity Deviation (1000 -100ke-) [rms%]	100 kpix/s			1	#TBD	+50e- max
CTE	100 kpix/s	#TBD	#TBD	0.999990	#TBD	min
Amplifier (Fullwell) [ke-]	100 kpix/s	#TBD		#TBD		
Blooming (Fullwell) [ke-/pix]		#TBD	#TBD	150	#TBD	min

Comment :

Readout Noise Error [rms e-] (ES0) : ± 0.2
 Conversion Factor Error [e-/ADU] (ES0) : ± 0.05

CTE Method used : EPER

Is updated by macro
 Not measured
 #TBD To Be Done

Figure III-3: Page three of the template for a CCD test report

Declaration on autonomy

Declaration on autonomy

I declare that this bachelor thesis is the result of my own and independent work. I have not used any other resources than the ones stated.

Garching bei München, 13.07.2009

Signature

Abstract

Driven by the strong will to answer today's questions of astronomy, ambitious projects in development at the European Southern Observatory (ESO) require the implementation of a large number of optical detectors in their instruments in the near future. Therefore the Charge Coupled Devices (CCDs) have to be tested and qualified individually on a test bench against the contractual specifications.

A new testing facility is described, designed to face the challenge of a rising number of detectors to be characterized in an automated way. The miscellaneous requirements concerning the setup are highlighted and the functionality of hard- and software as well as the interactions between are explained.

Finally a compact assembly is introduced, providing the possibility to automatically determine all major CCD parameters like quantum efficiency, conversion factor, dark current, charge transfer efficiency, read out noise, and cosmetic defects as well as specific, interactive measurements, that can be performed from a remote computer.

Keywords: CCD characterization, test bench, automation, optical detectors